æ

22. ENVIRONMENAL SENSING

17 June 2020

In order to survive, reproduce, and physiologically adjust in appropriate ways at the correct times, nearly all species constantly monitor their internal and external environments. Assessment of the outside environment usually involves multi-domain, trans-membrane proteins, with an external domain serving as an environmental sensor, and an internal domain transmitting signals to messenger proteins that transfer information in ways that elicit appropriate cellular responses. These signal-transduction (ST) pathways may involve multiple steps, but information exchange almost always involves a series of chemical and/or physical changes in the pathway participants. ST systems are central to the nervous systems of metazoans, but for unicellular species, they are the nervous system.

At the single-molecule level, ST processes are digital in the sense that each molecular participant exhibits a finite number of effectively discrete phenotypes, e.g., active vs. inactive conformational states. At the whole-cell level, such information will be distributed over all of the relevant ST molecules in the cell, providing a more accurate assessment of environmental states. Unraveling the issues at both levels is key to understanding the function and evolutionary properties of communication systems at the cellular level.

The three main challenges of all ST pathways are sensitivity, accuracy, and speed. First, external nutrient and signal concentrations are often in the μl range (Chapter 18), so cells have to make decisions based on encounters with small numbers of molecules. Second, each ST pathway is devoted to a specific environmental stimulus (or small set of them), the menu of which is very broad, including organic metabolites, inorganic nutrients, markers of pathogens, atmospheric gases, osmolarity, and antibiotics. With up to several dozen pathways operating simultaneously within the confines of single cells, avoidance of crosstalk among pathways is critical to maintaining coherent cellular responses. Third, the chemical systems involved must generate responses on appropriate time scales. Too slow a response can leave a cell in a compromised physiological state, but too rapid a response can be a major energy drain.

Because all of the central players in signal transduction are enzymes, understanding the operation of such systems requires an appreciation of the basic features of enzyme kinetics. But this is not enough. As reviewed in Foundations 19.1, the kinetics of simple one-enzyme systems are such that there is generally a smooth, hyperbolic relationship between substrate concentration and enzyme output. In contrast, ST pathways generally incorporate feedback mechanisms among the participating enzymes that collectively can yield much sharper responses of the whole

system to external ligand concentrations. In extreme cases, this amplification of external signals can lead to near switch-like behavior in phenotypic outputs.

ST systems invoke many evolutionary questions, most of which remain to be answered in a convincing fashion. First, as the accurate transmission of environmental information among chains of pathway molecules is key to signal transduction, the recurring theme of the evolution of cohesive molecular languages again becomes central. Second, because the recording and erasing of information is energy demanding, questions emerge about the critical threshold above which the gain in information is offset by the energetic cost of building and maintaining a communication system. Third, the innate capacity of many ST systems to generate populations of discrete alternative states at the individual level (in the absence of genetic variation) raises questions as to when such systems have been exploited by natural selection to operate as bet-hedging strategies, as opposed to being inevitable by-products of the structure of ST networks.

In the following pages, these issues will be explored mainly from the standpoint of bacterial ST systems, which owing to their simplicity have been studied in much more detail than the more complicated ST networks typically operating in eukaryotes. A broad overview of the biology of ST systems, more focused on eukaryotes, is given by Lim et al. (2015).

Bacterial Signal-transduction Systems

Relative to the complex ST systems of eukaryotes (below), those of bacteria typically have simple enough structures that their operational features can be dissected in detail. The simplest bacterial ST mechanism is the so-called one-component system, consisting of just a single protein (usually cytosolic) with an input domain serving as a signal receptor (sensor) and an output domain for transmitting information to a receiver (Figure 22.1). Almost always, the incoming signal is a small molecule that allosterically modifies the protein in such a way as to activate the response domain, which then induces transcription in one or more downstream genes (Ulrich et al. 2005).

The second most common mechanism of signal transduction in bacteria is the two-component system (Stock et al. 2000; Capra and Laub 2012), the operation of which always involves post-translational modification. The first component in such systems, the signal receptor, is generally a histidine kinase (HK) embedded in the cell membrane; kinases are enzymes that catalyze the transfer of a terminal phosphate from ATP to an amino acid. The extracellular domain of a HK receives environmental information, usually in the form of a small ligand that induces phosphorylation (addition of a phosphate group) of a specific histidine residue on the internal domain (Figure 22.1). The phosphoryl group is then transferred to a specific aspartate residue on the second (intracellular) component, known as the response regulator (RR) protein. This transfer elicits a conformational change in the RR that in turn induces a specific cellular response, usually with the RR operating as a transcription factor. Almost all HK and RR proteins have homodimeric structures.

There are thus six key determinants of specificity in a two-component system: the ligand-binding, phosphotransfer, and dimerization domains of the HK, and the

receiver, DNA-binding, and dimerization domains of the RR. Moreover, most HK proteins are bifunctional in that when not phosphorylated, they operate as phosphatases on their cognate RR proteins, with the ratio of kinase to phosphatase activity dictating the output of the pathway. In *E. coli,* an average HK protein is represented by 10 to 100 molecules per cell, whereas the cognate response regulators are generally 10 to 100× more abundant.

Some bacteria also harbor more complex phospho-relay systems, the simplest of which consist of three components (Figure 22.1). Again, a membrane-bound HK molecule first autophosphorylates at an internal histidine residue after receiving an appropriate extracellular signal. But in this case, the phosphoryl group is then transferred to a secondary receiver domain, often intramolecularly (to an arginine residue). Given the presence of both a transfer and acceptor domain in the same molecule, such a protein is often referred to as a hybrid kinase. A separate phosphotransferase protein transfers the phosphoryl group to the final acceptor, a cytosolic RR protein. A number of variants on this type of pathway are known, including chains of transfers from a histidine to an arginine to another histidine, and so on. The *Bacillus subtilis* sporulation control system is an example of a chain involving a series of four proteins (Sonenshein 2000).

Origin and diversification. The numbers of both one- and two-component systems in different bacterial species scale with roughly the square of genome size (Ulrich et al. 2005; Alm et al. 2006; Capra and Laub 2012). One-component systems are about 7× more abundant than two-component systems, with most bacterial species containing dozens (in a few cases, hundreds) of such systems in total (Figure 22.2). The HK and RR pairs in most two-component systems reside in the same operons, and hence are coexpressed. Nevertheless, many cases are known in which single members of an operon are duplicated, with the numbers of orphan HK and RR genes being nearly as abundant, on average, as those in operons (Burger and van Nimwegen 2008). In addition, although they are a minority, many-to-one and one-to-many HK-RR systems exist (Goulian 2010), with the numbers of HK proteins in a genome usually being between 1 and 2× the number of RR proteins (Figure 22.2). This implies that multiple signals are often transmitted through the same response regulator.

Given the very precise mode of operation of all such systems, an initial phosphorylation of a histidine on one protein, followed by phosphotransfer to an aspartate on another, it is likely that this was the ancestral state of an initial two-component system from which most others were subsequently derived by duplication and divergence. Why phosphorylation was settled upon as the key form of post-translational modification remains unclear, although the two negatively charged oxygens associated with each phosphate group provide numerous opportunities for the modification of protein structure by binding with positively charged residues. Such structural changes can then be linked to alterations in protein function in a binary fashion.

There are many parallels between one- and two-component systems (Ulrich et al. 2005). In ∼95% of both cases, information on the environment is acquired via small-molecule binding, and in ∼85% of cases, the output involves transcriptional regulation of target-gene expression. Many input and output domains appear to be shared between one- and two-component systems, with unique sensor domains

appearing only in the one-component group. Given the simplicity of one-component systems, this overlap motivates the suggestion that such simple systems provide the evolutionary seeds of two-component systems (Ulrich et al. 2005). However, any such transition would require several modifications: minimally, the insertion of a histidine kinase domain and a receptor domain, the physical separation of these two domains into two separate proteins, and the acquisition of a trans-membrane domain by the HK. Thus, there is no compelling reason to rule out the alternative possibility that one-component systems are derived and simplified from RR members of two-component systems.

Coevolutionary integration of components. The multiplicity of ST systems operating within individual cells and their operation by pairwise communication raise many questions about their evolutionary properties. One of the central issues concerns the mechanisms by which individual systems avoid the decision-making risks of miscommunication with noncognate systems. The degree of insulation between noncognate systems *in vivo* is typically quite refined, with each HK generally communicating with a specific RR, although some low level of error must occur. Indeed, some systems exhibit a low degree of crosstalk *in vitro* (Yamamoto et al. 2005), and crosstalk can be greatly enhanced if cognate partners are eliminated, owing to the release from competitive binding (Siryaporn and Goulian 2008).

Pathway insulation is in part an ingrained consequence of the biochemical nature of bacterial two-component pathways, in particular the editing-like properties of the HK molecules. When the proper signal for a particular pathway is lacking, its HK remains unphosphorylated and acts primarily as a phosphatase for the cognate RR, tending to erase inadvertent phosphorylation of an RR by a noncognate HK. When the proper signal is present, the cognate HK is phosphorylated at a high level, with any promiscuous phosphoryl transfer by a noncognate HK only serving to reinforce the signal.

This being said, there is still considerable potential for the rapid evolution of HK-RR specificity changes. Mutual HK-RR recognition of phosphotransfer sites is generally a function of coevolutionary changes accumulated on just a small number of amino-acid residues, typically < 6 sites on each protein (Li et al. 2003; Laub and Goulian 2007; Weigt et al. 2009; Capra et al. 2012b). Combined with the latent promiscuity noted above, this suggests that specificity rewiring may be readily accomplished with only a small number of single-residue changes. As an example, alterations of just three amino-acid residues of the *E. coli* HK EnvZ is sufficient to both eliminate its ability to recognize its cognate RR and to confer full specificity toward the noncognate RR RstA (Skerker et al. 2008; Capra et al. 2010). In this study, single amino-acid changes allowed mutual recognition of cognate and noncognate RRs, showing that under the right situations, a HK can gain an ability to recognize a novel RR without relinquishing its initial partner. Indeed, Siryaporn et al. (2010) found that single amino-acid substitutions in an *E. coli* sensor kinase called CpxA can cause the efficiency of signaling to a noncognate RR to even exceed that of the latter's cognate HK.

Observations like these highlight the potential for producing novel ST pathways by altering the communication language via just a small number of amino-acid modifications. A dramatic example of such evolutionary exploitation was found

in an experimental study of *Pseudomonas* in which the deletion of the flagellar regulatory gene abrogated swimming ability (Taylor et al. 2015). After just 96 hours of selection for motility, mutant strains were found to have acquired mutations in the two-component ST system normally involved in the regulation of nitrogen metabolism, redirecting its signal towards flagellum production.

In a broader attempt to understand the degree of recognition-motif degeneracy, Podgornaia and Laub (2015) made constructs of all possible 160,000 (20^4) amino-acid combinations for the four key recognition residues in *E. coli* protein kinase PhoQ, a signal receptor for external magnesium concentration, finding 1659 of them to be functional. Taking this kind of analysis even further to include the recognition motif on the cognate response regulator PhoP, McClune et al. (2019) found 58 unique PhoQ-PhoP motif combinations that not only yielded fully functional systems but were also completely insulated from the native system.

This ability to alter crosstalk via simple amino-acid module exchange in ST systems provides enormous opportunities in biotechnology for synthesizing novel environmental sensors. For example, bacterial histidine-aspartate phospho-relay systems can be fully expressed in mammalian cells, where tyrosine-serine-threonine relays are the rule, with functional interference being minimal (Hansen et al. 2014).

Given that many two-component systems operate in an essentially one-to-one manner, these kinds of observations also suggest the capacity for substantial neutral coevolutionary drift between interacting motifs, even in the face of selection for conserved function. Recalling the theory discussed in Chapter 21, such systems drift in coupled regulatory vocabularies in simple pairwise interactions is expected, so long as the maintenance of a strong degree of mutual interaction is retained (Lynch and Hagner 2015). In principle, this would then lead to incompatibilities among mixtures of orthologous HKs and RRs from different taxa.

The few experimental attempts to shed light on this matter have yielded mixed results. On the one hand, divergence of the recognition motifs of the components of the bacterial PhoR-PhoB system (involved in phosphate regulation) between the α and γ branches of the Proteobacteria is sufficient to nearly completely prevent crosstalk in foreign constructs (Capra et al. 2012b). On the other hand, two studies of other systems have shown that the HK gene from a different bacterial phylum can complement the loss of the orthologous *E. coli* gene (Tabatabai and Forst 1995; Ballal et al. 2002). Likewise, the conserved ability to phosphorylate orthologous substrate proteins from distantly related species has been noted for a different class of bacterial signaling proteins, the tyrosine kinases, in this case despite the lack of obvious sequence homology (Shi et al. 2014). These kinds of observations are not necessarily incompatible with a hypothesis of neutral systems drift, although it does highlight uncertainties in the degree to which the evolution of sequence motifs in the individual participants are mutually constrained.

Emergence of new pathways. These types of observations make clear that two-component systems can be rewired with only a small number of changes. But the challenges in establishing an entirely new ST system are numerous. A common idea is that the evolution of a novel system initiates with duplication of both members of the pair, a scenario made plausible by the frequent joint occurrence of cognate HK and RR genes in the same operon. However, ultimate preservation by neofunc-

tionalization requires the origin and integration of a new signal input and/or output into a system that avoids crosstalk with the ancestral system (Figure 22.3). This, in turn, requires divergence in the HK-RR communication language of parental and/or duplicate pairs so as to avoid unproductive crosstalk (Capra et al. 2012b). Evidence suggests that the amino-acid sequences within HK-RR interface regions evolve at high rates at least in the early stages of post-duplication divergence (Rowland and Deeds 2014), and dramatic changes in the recognition motifs are known to have accumulated among duplicated systems within the γ-Proteobacteria (Capra et al. 2012b). While these observations are potentially consistent with diversifying selection, it remains unclear whether they are inconsistent with a simple phase of neutral random genetic drift.

Moreover, modifications at the HK-RR phosphotransfer interface are not enough for the insulation of two pathways. There is also a need for changes in the dimerization interfaces of both the HK and RR molecules to prevent heterodimerization with ancestral copies. Experimental work again suggests that changes involving fewer than four amino-acid residues in dimerization interfaces can be sufficient to establish a new homodimerization group (Ashenberg et al. 2011).

Capra and Laub (2012) and Rowland and Deeds (2014) have suggested that all of these crosstalk interactions must be removed before new input/output functions are acquired, arguing that in large bacterial populations even mutations with very mildly deleterious crosstalk effects would be immediately removed by selection. If this is indeed the case, then a transition to a novel signaling pathway would require an early order of events that is essentially neutral with little to no impact on the overall output of the ancestral system.

The difficulty of this hypothesis is that the multiple steps that must be accomplished (two losses each of heterodimerization potential and cross-phosphotransfer potential, and the emergence of at least one new HK-RR phosphotransfer interaction) must also require substantial time, during which neither system can acquire a nonfunctionalizing mutation (which would remove the entire system from selection). It may help that most bacterial populations are so large that most first-step variants (as well as double mutants) are always maintained by recurrent mutation; these can then provide the staging grounds for the emergence of downstream mutations, which can then proceed to fixation without any bottleneck in population fitness (Chapter 5). Suffice it to say that the population-genetic conditions necessary for the emergence of an insulated, coevolving pair of proteins will have to be worked out to resolve these numerous open questions.

Despite all of these caveats, a high degree of congruence between the phylogenetic trees of HK and RR genes conjoined within operons is consistent with the hypothesis that HK-RR pairs frequently arise by operon duplication (Koretke et al. 2000). Linkage within operons ensures that both members of the pair will be coexpressed from their time of origin, an essential ingredient for coevolution.

Finally, a plausible case can be made that more complex phospho-relay systems (Figure 22.1) arise by fusion of the HK and RR components of two-component systems. In principle, this may involve nothing more than deletion of an intergenic region within an operon, provided the open-reading frames of both components intact (Zhang and Shi 2005; Cock and Whitworth 2007). Such a starting point would facilitate the evolution of a new signaling system, as the HK and RR are

already open to communication. In addition, their enforced proximity within the same molecule would reduce the necessity of high affinity between the pair, thereby enhancing the likelihood of evolutionary motif divergence. Consistent with this idea, empirical work has shown that when the kinase domain of a phospho-relay system is disconnected from its receiver domain, the level of crosstalk increases substantially (Wegener-Feldbrügge and Søgaard-Andersen 2009; Capra et al. 2012a). Once established with novel communication motifs with little potential for crosstalk, such a phospho-relay system might then revert back to the structure of a two-component system by a fission event.

Interconvertible Proteins and Ultrasensitivity

Despite their relatively simple modular structures, ST pathways exhibit an array of unusual features at the biochemical and cellular level. Central to most such systems are interconvertible proteins whose active vs. inactive states are defined by the presence/absence of post-translational modifications, as in a response regulator (RR) in a two-component system. As already discussed, the most common case by far is the phosphorylation/dephosphorylation cycle, in which a specific ATP-dependent kinase attaches a phosphoryl group to a particular amino-acid residue on the interconvertible protein, and a specialized phosphatase is responsible for the reverse reaction. In the simplest bacterial systems, the same enzyme is often used for both the addition and removal of the modification, but in eukaryotes different enzymes are generally deployed in each transformation. Operating simultaneously, the joint activities of kinases and phosphatases, along with the concentration of the intermediate protein, determine the fractional activity of the latter, which ultimately dictates the cellular response.

In the following discussion, the three enzymes will be denoted as F (forward converter, e.g., a kinase), R (reverse converter, e.g., a phosphatase), and I (interconvertible, e.g., a response regulator) (Figure 22.4). Although such systems have discrete on/off states at the single-molecule level, this is not the case for the entire ensemble of molecules at the cellular level. Instead, the relative levels of alternative forms of I (active $\mathrm{I_a}$, and inactive $\mathrm{I_i}$) can fall over an essentially continuous range of 0.0 to 1.0, depending on the activities of the converter enzymes (F and R). In one range of parameter space, the forward (kinase) reaction will dominate, and the majority of I will exist in its active form, whereas for other parameter values, the reverse (phosphatase) reaction will dominate, rendering the average molecule of I inactive.

A key question is how the fractional activation of I depends on the concentration of the external signal, the forward ligand $\mathrm{S_F}$, as this will dictate the magnitude of the overall cellular response. Recall that with standard Michaelis-Menten enzyme kinetics, there is a fairly gradual response of the system output to the substrate concentration (Chapter 19). However, with this triad of interacting proteins, more than ten parameters, including the kinetic parameters of enzymes F and R, determine the partitioning of the total concentration of I, denoted $[\mathrm{I_T}]$, into its active and inactive forms (Figure 22.4; Foundations 22.1). As a consequence, the level of I activation can exhibit a far richer array of behaviors than possible with basic enzyme kinetics,

even though both enzymes F and R behave as Michaelis-Menten enzymes with I as their substrate.

Consider the situation in which the active vs. inactive form of converter enzyme F depends on whether it is bound to its ligand S_F (Figure 22.4), and recall that with Michaelis-Menten enzymes, the rate of a reaction is hyperbolically related to the substrate concentration, $[S_F]$. With increasing $[S_F]$, enzyme F is expected to be increasingly converted to its active form F_a. If, however, F_a feeds into a loop involving the interconvertible enzyme I, the fraction of active enzyme, $I^* = [I_a]/[I_T]$, can reach much higher levels than the fraction of active F at low levels of the input substrate S_F (Figure 22.5, upper panel). In other words, the signal from the external ligand can be substantially amplified. This is because the total concentration of I constitutes a closed system, enabling F_a to cumulatively convert I_i to I_a.

The degree of amplification depends on the kinetic parameters of the reverse converter, which provides the only route back to I_i. As the forward conversion reaction increasingly overwhelms the reverse reaction, the phosphorylation reaction dominates, and $I_a \rightarrow I_T$. On the other hand, as the kinetic efficiency of enzyme R increases, the phosphatase reaction increasingly dominates, and the system can converge to situations in which I can never attain a fully active state, even at the highest concentrations of the external ligand (Figure 22.5, upper panel).

A key assumption underlying the preceding results is that the total concentration of I is substantially below the half-saturation constants for the forward and reverse reactions (Stadtman and Chock 1977), so that the active forms of enzymes F and R are not saturated by their substrate. In this case, a simple expression can be obtained for the fraction of activated intermediate enzyme,

$$I^* = \frac{\kappa_F[F_a]}{\kappa_R[R_a] + \kappa_F[F_a]}, \tag{22.1}$$

where κ_x is the kinetic efficiency of enzyme x operating on substrate I (from Equations 22.1.7a,b). In this nonsaturating case, the forward and reverse rates of conversion of *I* are both linearly related to their substrate concentrations, and I^* is independent of the total concentration of intermediate enzyme, $[I_T]$, in the system. Furthermore, because the amounts of active converter enzymes, $[F_a]$ and $[R_a]$, are Michaelis-Menten functions of their ligand concentrations (Equations 22.2.3a,b), I^* is also a conventional hyperbolic function.

Goldbeter and Koshland (1981) found that with increasing concentration of I in the system (so that the responses of F_a and R_a to their substrate concentrations are no longer linear), the response of I^* to ligand concentrations is no longer hyperbolic or independent of $[I_T]$. Rather, the steepness of the activation response to ligand concentrations elevates dramatically with increasing $[I_T]$, in the extreme becoming an effectively stepwise process (Figure 22.5, lower panel). This sharp response is often referred to as zero-order ultrasensitivity. Such behavior arises because high levels of I allow the converter enzymes to operate at maximum capacity, thereby sharpening their responses near the threshold between the kinase and phosphatase domains on the scale of ligand concentrations. At low levels of the external ligand, the reverse (phosphatase) reaction dominates, and with a high level of I pushes the rate of a conversion to I_i to the maximum. At high levels of the external ligand, the forward reaction dominates, pushing I_a to the maximum level.

To summarize, the use of an interconvertible-enzyme system can alter both the sensitivity and the amplitude of response of a signaling system to the input ligand concentration. Most notably, for sufficiently high concentrations of the central enzyme I, near switch-like behavior of the population of active I molecules arises. Thus, should a selective scenario exist in which switch-like behavior is advantageous, mutational fine tuning of the kinetic parameters of the enzymes underlying the ST system, combined with the maintenance of a high level of I, can provide an evolutionary path towards such behavior. Significantly, with signal transduction driven by kinase/phosphatase enzymes capable of modifying hundreds of substrate molecules per second, much more rapid shifts in cellular states can be achieved than by changes in the level of gene expression.

Here, it should be emphasized that whether the switch-like behavior implied by the mathematics of these kinds of systems commonly occurs in cells, let alone is promoted by selection, remains an open question. In fact, zero-order ultrasensitivity has not yet been directly demonstrated in *in vivo* signal-transduction systems (Blüthgen 2006). Moreover, as pointed out by Ortega et al. (2002) and Xu and Gunawardena (2012), such an extreme response requires that the phosphorylation/dephosphorylation reactions are intrinsically irreversible, such that a predominating kinase can literally drive I to the point at which all molecules are in the active state. With most enzymes, a high product concentration generally drives reactions in their reverse direction, leading to an equilibrium situation in which both active and inactive molecules coexist within a cell. The situation is even more complicated in bacterial two-component systems, where the same enzyme ofte serves both the F and R functions, which renders the maintenance of high substrate concentrations for both enzymatic functions (necessary for ultrasensitivity) difficult to achieve. Thus, it remains uncertain whether the kinds of extreme behavior displayed in Figure 22.5 are ever approached in natural systems, although as discussed below, cells can indeed exhibit switch-like behavior at the phenotypic level.

The cost of signal transduction. Acquisition, processing, and propagation of information requires energy, whether via a computer (Landauer 1988) or by the nervous system of a metazoan (Niven 2016). Even quiescent nerve tissue consumes energy just to maintain a steady response capacity. The same is true for the interconvertible enzymes at the heart of ST systems. There are structural costs in terms of the maintenance of the converter enzymes and their interconvertible substrate I. In addition, to provide information on the external environment, the relay signal (the relative concentrations of active and inactive I molecules) must be constantly adjusted by the simultaneous running of two pathways (phosphorylation and dephosphorylation) in opposing directions. For this reason, the dynamics of interconvertible proteins outlined above are often referred to as push-and-pull or futile cycles – even when the system settles into a steady-state in a constant environment, active and inactive I molecules are continuously being interconverted, leading to a cyclical flux.

Because each activating phosphorylation event requires the expenditure of an ATP molecule, a rough idea of the cost of maintaining such an intermediate protein at a particular level of activity can be obtained by noting that at steady state, the reciprocal rates of activation/inactivation of I molecules must be completely

balanced, and that this rate must also equal the rate of ATP consumption. The latter prediction has been verified empirically (Shacter et al. 1984). Again, defining $I^* = [\mathrm{I_a}]/[\mathrm{I_T}]$ to be the fraction of the interconvertible enzyme in the active state, and recalling that the reverse converter operates on activated molecules in a Michaelis-Menten way, the rate of ATP consumption can be directly acquired from the formula for the rate of conversion of active to inactive enzyme. Dividing all terms on the right of Equations 22.1.4a,b by $[\mathrm{I_T}]$ yields alternative expressions for the rate of ATP consumption necessary to maintain the system at a fractional level of activated protein,

$$V_{\mathrm{ATP}} = \frac{k_{\mathrm{cat,R}}[R_\mathrm{a}][\mathrm{I}^*]}{k_\mathrm{R}^* + [\mathrm{I}^*]} = \frac{k_{\mathrm{cat,F}}[F_\mathrm{a}](1-[\mathrm{I}^*])}{k_\mathrm{F}^* + 1 - [\mathrm{I}^*]}, \tag{22.2}$$

where $k_\mathrm{R}^* = k_{S,\mathrm{R}}/[[\mathrm{I_T}]$ is the scaled half-saturation constant for the reverse converter, and similarly for k_F^*. Note that the rate of ATP consumption is a hyperbolic function of I^*.

Thus, estimates of the cost of running a signal-transduction system can be obtained from measures of *in vivo* rates of ATP consumption by the pathway kinases. For example, Shacter et al. (1984) noted that the flux through hepatic pyruvate kinase is $V_{\mathrm{ATP}} = 20$ to $200\,\mu$M/min, depending on the level of activation of the intermediate protein. Assuming a cell volume of $\sim 5000\,\mu\mathrm{m}^3 = 5 \times 10^{-12}$ liters, a cell division time of ~ 24 hours, and converting moles to number of molecules using Avogadro's number, the total rate of ATP consumption by this kinase is then $\sim 10^{10}$ to 10^{12} molecules/cell cycle. Estimates for other mammalian kinases derived in Goldbeter and Koshland (1987) are in this rough range as well. A quantitative understanding of what this energetic cost means to the cell requires information on the total cellular energy budget. From Chapter 8, for a cell of this size and cell-cycle length, total cell maintenance costs are $\sim 2 \times 10^{13}$ ATP hydrolyses/cell cycle, implying that a single mammalian ST system can demand up to 5% of a cell's energy budget.

Similarities and differences in eukaryotic systems. Eukaryotic signal transduction systems are generally much more complex than those in bacteria. Although kinases and phosphatases are still broadly utilized, different amino acids serve as the usual sites of phosphorylation – serine, threonine, and tyrosine, the latter largely confined to metazoans. Whereas bacterial histidine kinases produce phosphoramidates by phosphorylating side-chain nitrogen atoms, eukaryotic phosphorylate serine, threonine, and tyrosine kinases creating phosphoesters by linking with oxygen atoms, which are much more energetically stable. Perhaps this stability is essential for activated molecules that have to travel larger distances in eukaryotic cells.

The numbers of kinases scale with roughly the square of the total number of proteins, similar to what is seen in bacteria, and substantial lineage-specific expansions of particular families have arisen (Anantharaman et al. 2007). Some two-component systems involving autophosphorylating histidine kinases are known in plants, fungi, and slime molds, but they are absent from a number eukaryotic lineages, notably metazoans (Loomis et al. 1997; Schaller et al. 2011). Moreover, in eukaryotes, each of the interacting enzymes typically engages with multiple substrate proteins (Figure 22.6), often more than a dozen, leading to complex networks quite unlike the

well-insulated systems of bacteria. Hence, the elegant molecular dissections that have been done for bacterial ST systems are a rarity for eukaryotes.

Nonetheless, for the few simple systems that have been investigated, many of the principles outlined above for bacteria with respect to motif evolution still apply. For example, a transcription factor involved in the response to amino-acid starvation in the yeast *S. cerevisiae* (Gcn4) is targeted for degradation by a specialized kinase (Pho85), but whereas the same system operates in the yeast *Candida albicans,* the cross-species components are incapable of molecular recognition (Gildor et al. 2005). As discussed above for bacteria, this kind of coevolutionary wandering of the motif language used in information transfer in the face of conserved function is consistent with the operation of mutually constrained systems drift.

There can, however, be limits to the degree to which such wandering can extend. For example, Zarrinpar et al. (2003) found that a kinase (Pbs2) involved in the osmoregulation pathway in *S. cerevisiae* interacts specifically with one membrane-bound sensor protein, despite the presence in this species of 26 other related proteins with rather similar recognition sequences. However, when orthologs of these off-target proteins from other distantly related species were presented to Pbs2, strong recognition often occurred. This suggests that there has been strong negative selection within yeast to avoid off-target interactions.

Contrary to the situation in bacterial ST systems where just a single amino-acid residue is typically modified on the intermediate protein, eukaryotic proteins commonly have multiple phosphosites. Because the activity of the modified enzyme can require a complete set of phosphorylated sites, and the sequential ordering of marks may follow a rigid recipe, this introduces novel twists to the types of models discussed in the preceding section. Contrary to the switch-like behavior found with simple systems with single-site modifications, the use of multiple phosphorylation sites for activation leads to a more graded response. Although there is still a threshold level of substrate below which the system is inactive, there is a simple Michaelis-Menten-like response above the threshold (Gunawardena 2005). Thus, although the reason for the use of multiple phosphosites in eukaryotic ST-pathway enzymes remains unclear, refined enhancement of switch-like behavior does not seem to be a viable hypothesis.

Limited attention has been given to the consequences of the kinds of shared utilization of kinases/phosphatases illustrated in Figure 22.6 (left). However, focusing on the simple case of enzymes with single modifiable sites, Rowland et al. (2012) found that coupled systems can often behave in a transitive fashion, such that if one intermediate substrate saturates the controlling enzymes in a way that leads to switch-like ultrasensitivity, all other connected intermediate enzymes will behave in the same way. In effect, saturation by one intermediate substrate alters the controlling enzymes (F and R) to fully active states, governing the entire system. This can even happen when all of multiple intermediate substrates are below saturation levels, provided the aggregate is sufficient for saturation. Whether these kinds of collective effects are evolved mechanisms for coordinated ultrasensitivity in eukaryotic cells remains unclear, given the typical use of multiple phosphosites in such organisms and the consequences just noted.

One of the most pronounced differences between eukaryotic and bacterial ST systems is the extended length of the former, with a relay of three kinases being

particularly common (Figure 22.6, right). For example, MAP kinase kinase kinases phosphorylate MAP kinase kinases, which in turn phosphorylate MAP kinases that finally transmit information to a response regulator. Many variants of the MAP kinase family exist, with their efficiency of operation and degree of insulation being enhanced by the use of scaffold proteins that effectively link all three layers of each pathway into single complexes. How and why pathways with extra steps evolve remains unclear, but Armbruster et al. (2014) argue that added steps enable pathways to integrate out the effects of environmental noise on the elicited response.

Given that eukaryotes are derived from the archaea, it is of interest to know the nature of ST systems in the latter. There is an unfortunate void of knowledge here, although it is known that many archaea are entirely lacking histidine kinases, and that perhaps all have serine/threonine kinases (Makarova et al. 2017). What is most unusual is the apparent exploitation of KaiC-like ATPases in a wide variety of signaling pathways across the archaeal phylogeny. Recalling from Chapter 18 that KaiC is at the heart of the phosphorylation/dephosphorylation cycle that forms the circadian clock in cyanobacteria, this suggests the possibility that the latter may have been acquired by horizontal transfer from archaea.

Finally, it is worth recalling that eukaryotes harbor another broad class of proteins largely addressed towards intracellular messaging, the so-called G proteins, used in a wide range of cellular activities, including vesicle transport and import/export through nuclear pores (Chapter 15). Although these proteins operate in a quite different way than those noted above, through binding of GTP rather than via phosphorylation of amino acids, the kinetics of the overall systems follows the same general plan as noted above for the interconvertible proteins involved in signal transduction. G proteins have alternative on/off states being driven by opposing enzymes responsible for GTP addition and removal, which in turn lead to conformational changes in the substrate G protein: writers called guanine nucleotide exchange factors (GEFs) add GTP to the G protein putting it in the active state; whereas erasers called GTPase-activator proteins (GAPs) hydrolyze the GTP to GDP, rendering the G protein inactive. Most GEFs are membrane-bound G-protein-coupled receptors (GPCRs) that become activated GEFs upon binding an appropriate ligand, thereby presenting a still further analogy with the types of systems noted above.

Chemoreception

There are just a few ST systems in bacteria more complex than the two-component systems noted above, the most ornate being that involved in chemotaxis, which directs motility towards particular chemo-attractants (or away from repellants). Although such systems have a kinase and a response regulator at their core, the output of the system is modulated by up to nine other participants (Figure 22.7). Rather than being membrane-bound, the histidine kinase, CheA, is located at the base of a sensory complex, connected by a linker protein to a special set of chemoreceptors (called methyl-accepting chemotaxis proteins or MCPs) found at the cell surface. Rather than operating as a transcription factor, the response regulator, CheY, interacts directly with the base of the flagellum, immediately causing a change in

swimming behavior. This allows for a much more rapid response than with conventional two-component systems that regulate gene expression. Specialized methyltransferases and methylesterases regulate the methylation level of four key residues on the MCPs, endowing them with a capacity for what is commonly referred to as adaptation, i.e., an ability to modify the ligand uptake kinetics in ways that stabilize the level of sensitivity over a broad range of concentrations of the external ligand.

Although the complex kinetic and dynamical features of the *E. coli* chemotaxis system have been worked out in considerable detail (Barkai and Leibler 1997; Keymer et al. 2006; Mello and Tu 2007; Bitbol and Wingreen 2015; Colin and Sourjik 2017), these technicalities will not be covered here. The key point is that bacterial chemotactic responses are achieved by cell's ability to compare current a ligand concentration with that in the recent past, reflected in part by the level of receptor methylation. High levels of methylation result from high levels of ligand concentration, but this decreases ligand affinity, in effect re-sensitizing the system to higher levels of chemoattractant that would otherwise be saturating. As a consequence of this negative feedback, in a stable environment, regardless of the ligand concentration, the activation level of CheA also remains stable, enabling the cell to maintain a constant sensitivity to changes in ligand concentration (analogous to the way in which the vertebrate eye adjusts to different levels of light).

Transmission of information from the external ligand concentration to the modified response regulator is accomplished through the response mechanisms noted above, in this case with CheA and then CheY becoming phosphorylated in the absence of ligand binding. The switch dictates whether the flagellum rotates in a clockwise (CheY bound when phosphorylated) vs. counterclockwise (CheY unbound when dephosphorylated by phosphatase CheZ) fashion, the former causing tumbling and a change in direction, the latter propelling the cell forward. This sort of guided behavior then leads to a biased random walk in the direction of a perceived chemical gradient.

The MCPs typically sit in one or two large hexagonal arrays at the cell surface, organized in a honeycomb-like form; 1000 to 15,000 trimers of receptor dimers form the vertices and act as relays to the histidine kinase, CheA (Briegel et al. 2009). In *E. coli,* there are five forms of MCPs, with various sensitivities to different amino acids and sugars. As the different types are mixed together within the arrays, this allows the cell to simultaneously process complex information about the environment. Cooperative interactions between adjacent elements sharpen the response (Mello et al. 2004). Absent from eukaryotes, this type of chemotaxis system appears to have been horizontally transferred to some archaeal lineages (Briegel et al. 2015), even though the archaeal flagellum appears to have evolved independently (Chapter 16).

Approximately 50% of bacterial species have a chemotaxis system, although the architectural features vary widely, with some having as few as three additional proteins outside of the core CheA and CheY (Wuichet and Zhulin 2010), and others having additions (Abedrabbo et al. 2017). Whereas *E. coli* has five types of receptor proteins, the number ranges from 1 to 30 in other bacteria (Wadhams et al. 2005). A clear example of the evolutionary rewiring of such systems is revealed by the contrast between the *E. coli* network, described above, and that in the soil bacterium *Bacillus subtilis.* For example, whereas interaction of CheY-P with the flagellar motor induces clockwise rotation and tumbling in *E. coli,* it induces counterclockwise

rotation and directional swimming in *B. subtilis;* and whereas the phosphatase CheZ dephosphorylates CheY-P in *E. coli,* this function is carried out by a flagellar motor protein in *B. subtilis* (Szurmant et al. 2004; Yang et al. 2015). The purple photosynthetic bacterium *Rhodobacter sphaeroides* has nine different receptor proteins, as well as four versions of CheA and six of CheY, which crosstalk in nonrandom ways, presumably broadening the level of environmental differentiation made possible by this system (Porter and Armitage 2002, 2004).

Chemotaxis enables organisms to move up resource gradients, thereby leading to an elevation of individual reproductive rate. However, the accrued advantage may be more nuanced. In an otherwise homogeneous environment, at the edge of its range, populations of organisms will indirectly generate a gradient of a chemo-attractant through their own activities, thereby causing continued migration (Adler 1966). Cremer et al. (2019) found that under conditions in which resources are nonlimiting to growth, *E. coli* still migrate towards a chemo-attractant of no nutritional value. This leads to range expansion, which increases the ultimate overall growth rate, as the migrating cells at the leading edge expand the clonal range over a greater area, while the laggards fill in the space behind and utilize the still plentiful nutrients. Clones modified to be insensitive to chemo-gradients experience lower overall growth rates because more cells experience local resource limitation.

Notably, if the attractant is the primary nutrient, this effect is not seen – if the attractant/nutrient is nonlimiting, the strong self-produced gradient necessary for expansion does not occur, and if it is too limiting, the migrating wave depletes the nutrients remaining for any laggards. Thus, although the usual view is that chemotaxis has evolved as a mechanism for moving towards more beneficial conditions, the authors of the preceding study suggest a role for simply expanding into unoccupied locations even under nutrient replete conditions. Whether the benign conditions necessary to drive such a process commonly exist in nature is unclear, and perhaps questionable. In addition, the kinds of spatial structure that can arise on a completely unoccupied solid surface do not readily generalize.

Indeed, when *E. coli* is grown in a well-mixed liquid environment (which prevents the development of chemical gradients), cells increase their investment in motility when grown in nutrient-poor environments, consistent with the idea that such a shift is a searching mechanism for more nutrient-rich environments (Ni et al. 2020). Notably, laboratory populations of *E. coli* exhibit higher levels of chemotaxis towards amino acids that serve as more nutritional resources, although such a correlation does not exist for *B. subtilis* (Yang et al. 2015). Such mixed results may exist because utility in a laboratory setting need not reflect the conditions under which differential chemosensitivity evolved in nature. For example, whereas amino acids are commonly used as nutrients in the intestinal bacterium *E. coli,* they may simply serve as indicators of other resources in the soil bacterium *B. subtilis.*

Outside of issues related to cell migration and signaling in metazoan development, much less attention has been given to the mechanisms of chemotaxis in eukaryotes, the best example coming from the slime mold *Dictyostelium discoideum.* Unlike small bacteria, whose arrayed chemoreceptors monitor nutrients in a temporal manner, larger eukaryotic cells populate their entire surfaces with receptors and are able to sense spatial concentration gradients of $< 5\%$ from the front to the rear of the cell (van Haastert and Postma 2007).

During times of nutrient scarcity, these amoeboid cells aggregate into multicellular slugs, with recruitment being induced by waves of cyclic AMP emanating from the aggregation center about every 6 minutes. Cells respond by producing pseudopods in the direction of the fronts of waves, and continue to do so even after the wavefront has passed and the gradient has shifted direction. Skoge et al. (2014) found that the solution to this "back of the wave" problem is embodied in network principles associated with memory-like processes associated with positive feedback. As a wave approaches, the front of the cell is sensitized, whereas the back is desensitized, and the message to move forward persists for several minutes owing to the slow decay of the positive-feedback mechanism. The kinetics of the response system have clearly coevolved with the response system, as exposure to waves with periodicities exceeding 6 minutes leads to reversals in migratory behavior.

Finally, as noted above, the maintenance of the information endowed by ST systems requires energy. Govern and ten Wolde (2014) have estimated that in *E. coli* the opposing processes of phosphorylation and dephosphorylation consume $\sim 3 \times 10^7$ ATP hydrolyses per hour, which is $\sim 4\%$ of the total operating costs of the flagella during swimming (Schavemaker and Lynch, in prep.) Additional ATP must also be consumed in the opposing methylation and demethylation reactions operating on the MCPs.

Accuracy of environmental assessment. To improve fitness, the environmental sensing mechanisms of cells must provide accurate estimates of the concentrations of relevant ligands in the surrounding medium. The information to make such assessments is believed to reside in the degree to which signal receptors on the cell surface bind to their ligands. However, the former is an inherently stochastic process, owing to fluctuations in molecular arrival times and binding success at individual receptors. These problems were first analyzed by Berg and Purcell (1977), who showed how the degree of occupancy of a receptor can viewed as a counting mechanism for assessing ligand concentrations (Foundations 22.2).

Considering the features of a single receptor molecule, the basis for their result is the fact that the long-term average occupancy of a receptor is described by the Michaelis-Menten function $p = c_0/(K_D + c_0)$, where c_0 is the environmental concentration of the ligand, assumed to be momentarily constant, and K_D is the dissociation constant, equivalent to the concentration at which the receptor has a 50% probability of being bound. Note that for low ligand concentrations, $c_0 \ll K_D$, the relationship between p and c_0 is essentially linear, but with increasing c_0, the expected degree of occupancy approaches saturation (i.e., $p \simeq 1.0$). Thus, to be most effective in transmitting information, a receptor should have a dissociation constant larger than the typical environmental concentration. However, owing to the transient nature of binding, individual receptors have binary states at any particular time (bound or unbound), with only the long-term average providing a precise measure of p. Thus, accurate information on the degree of occupancy requires a long enough time for the averaging of repeated instances of binding and unbinding.

Assuming the cell continuously monitors the environment for a time period T, Berg and Purcell's estimated error in inference of the true environmental concen-

tration (c_0) is given by the coefficient of variation (CV)

$$\frac{\sigma_c}{c_0} = \sqrt{\frac{1}{2Dsc_0(1-p)T}}, \tag{22.3}$$

where D is the diffusion coefficient for the ligand, s is the radius of the receptor at the cell surface (the target size), and p is a function of c_0 defined above. This expression assumes that the process of information gathering is diffusion limited, i.e., once a receptor encounters a ligand molecule, it is a perfect absorber of that molecule. The full derivation of this expression is given in Foundations 22.2, but its final structure meets intuitive expectations. The level of noise in assessment scales negatively with the encounter rate and time, but positively with the degree of occupancy p. The quantity $4Dsc_0$ is the rate at which a ligand particle diffuses to a receptor. A longer T means that the receptor can integrate information over a longer series of bound and unbound states. As $p \to \infty$, the surface receptor becomes saturated, providing little quantitative information on the environmental state. As noted in Foundations 22.2, given typical estimates of D, even for quite low ligand concentrations, a measurement duration of several seconds can be sufficient to reduce the CV to a level near 0.01, i.e., to a level of $\sim 99\%$ accuracy in the estimation of the true environmental concentration.

The measurement of accuracy described by Equation 22.3 is based on just one of many possible ways in which a receptor might monitor the environment, in this case a time-averaged fractional occupancy of receptors. Endres and Wingreen (2009) showed that if the cell were somehow able to sense the duration of unbound intervals and use this alone as an estimate of c_0, the uncertainty in Equation 22.3 would be reduced by a factor of $1/\sqrt{2}$. Their argument is that only the length of unbound periods provides information on the environmental concentration of ligand. An alternative might be that the "counter" resides within the cellular interior, in which case the result in Equation 22.3 would need to be multiplied by 1.6 (Berg and Purcell 1977); the noise is elevated in this case because molecules transiently trapped within the cell (as opposed to being released into the environment) can be recounted, effectively reducing the number of independent evaluations per unit time. Finally, whereas both preceding calculations assume that the cell is evaluating a constant environment, gradient sensing (i.e., monitoring the rate of change of ligand concentration, as in swimming up a gradient, or contrasting the inferred concentration at two ends of a stationary cell) might be employed. Endres and Wingreen (2008) found that gradient sensing at the cell surface yields a measure identical to Equation 22.3, whereas monitoring inside the cell leads to a $2.9\times$ increase in the noise level, again emphasizing the advantages of monitoring at the cell surface.

All of these measures ignore the biochemical aspects of binding to receptors, making the assumption that the whole process is essentially diffusion limited; the necessary refinement for including the former is described in Foundations 22.2. In addition, it should be emphasized that the measure of noise outlined here does not necessarily translate linearly to the level that would emerge after transmission to the downstream signaling level; expressions that extend to this level have been introduced by Mehta and Schwab (2012).

Questions also remain as to the optimal spatial configuration of collections of sensor molecules (Iyengar and Rao 2014). On the one hand, spatial clustering re-

duces the sampling error in the vicinity of the array, but on the other hand, the spreading of receptors improves average sensing in spatially variable environments. Even in an environment that is spatially uniform on the scale of the length of the cell, sensor aggregation would enhance the conveying information into the cellular interior if cooperative interactions existed among adjacent receptor molecules, as appears to be the case for bacterial sensor arrays. With multiple receptors per cell (Briegel et al. 2009), averaging the information gleaned over all receptors will improve the accuracy to a degree that depends on the cooperativity among receptors, which remains to be determined. With n effectively independent receptors, this would just enter as a multiplier in the denominator of Equation 22.3. With cooperation among receptors, the denominator would have to be multiplied by n^x with $x > 1$.

There remain many unanswered evolutionary questions in this area. What is the optimal allocation of resources to environmental sensors in balancing the costs of production of such molecules and the advantages accrued? To what extent does the investment in sensing increase with increasing variance in environmental states? At what point does the energetic cost of the constant jostling of states of interconvertible enzymes offset the advantages of an ability to track environmental changes, to the point at which sensory overload necessitates the evolution of a constitutive general-purpose genotype? What role does the timescale of environmental fluctuations (e.g., within vs. between generations) play in these processes? Theory from a variety of angles relevant to these questions can be found in Lynch and Gabriel (1987), Lan et al. (2012), and Govern and Ten Wolde (2014).

Phenotypic Bimodality and Bet Hedging

ST systems provide a means for physiological acclimation within the lifespan of an individual cell. An alternative mechanism for dealing with environmental stochasticity is to generate phenotypic diversity independent of current environmental information. Here the focus is not on genetic polymorphism, but on the production of variable offspring by individual genotypes. This second option provides a potential advantage in that a segment of a clonal population can be immediately prepared upon an environmental shift, but this comes at the cost of another segment of the population being maladapted. Moreover, the possibility exists that all phenotypes are suboptimal. If phenotypic diversification among clonal progeny is to be promoted by natural selection, it must increase the long-term genotypic growth rate relative to that in other clones.

Although phenotypic distributions of biological traits are generally continuous in form (Lynch and Walsh 1998), striking cases of discrete bimodal states are known in microbes, e.g., dispersing vs. sedentary states, vegetative reproduction vs. spore formation, and activation vs. silencing of metabolic pathways. In some situations, different lineages of genetically identical cells can become trapped in alternative states for indefinite periods, even after the initiating environmental signal has dissipated, a condition known as hysteresis. There are a number of ways by which such phenotypic switching can be modulated by the types of ST pathway architecture noted above.

Consider the case of ultrasensitivity illustrated in Figure 22.5. Should cells straddle the threshold point, either because of stochastic internal cellular variation (e.g., molecular inheritance and/or transcriptional noise) or external environmental variation in ligand concentrations, individuals would receive entirely different messages for downstream phenotypic modification. In other words, adding noise to the otherwise deterministic model noted above will lead to some level of phenotypic switching. In this case, the duration of stays in alternative states would depend on the magnitude of fluctuations and the degree to which they are sustained.

Scenarios for the development of more sustained bimodality arise when there is positive feedback between the activated intermediate substrate and its activation enzyme, as shown graphically in Figure 22.8. In the absence of feedback, the rate of activation of the intermediate substrate (I) declines smoothly to 0.0 as the fraction of activated intermediate enzyme (I^*) approaches 1.0. With the rate of deactivation increasing smoothly with increasing I^*, a single intersection between these opposing functions leads to a single stable equilibrium point for I^* (Figure 22.7, left). When I^* exceeds this point, the rate of deactivation exceeds that of activation, and I^* declines, and vice versa if the starting point is below the equilibrium.

If, however, there is positive feedback between I^* and the activating enzyme, the form of the activation function can be altered in such a way that there are up to three alternative equilibria for I^* (Figure 22.8, right). When I^* is sufficiently low, increasing I^* further accelerates its own production by positive feedback, but eventually the rate of activation must decline, owing to the reduction in inactivated substrate. (Such positive feedback can also occur if I is a multimeric enzyme, requiring the assembly of multiple activated subunits for full functionality).

The key point is that positive feedback leads to an inflection in the activation function. If this function has three intersections with the deactivation function, the intermediate equilibrium will be unstable, as deviations in either direction result in movement towards the adjacent equilibria, both of which are stable. Thus, depending on their starting states, cells will gravitate towards one or the other alternative stable states, and remain there until fluctuations in the internal and/or external environments shift I^* into an alternative basin of attraction. Such a system is said to exhibit bistability. Assuming the different equilibrium levels of I^* are sufficient to lead to altered downstream patterns of gene expression, bistability of an underlying ST system provides a basis for eliciting discrete differences in phenotypic states of otherwise genetically identical cells. The relative frequencies of alternative states will depend on the underlying enzyme kinetics of the system and the magnitude and frequency of fluctuations in the governing parameters.

Bistability can arise under a number of other scenarios, including those involving inhibition, provided the number of inhibitory steps is even. If, for example, I_a inhibits the reverse enzyme, while I_i inhibits the forward enzyme (Figure 22.4), a situation then arises in which of the modifying enzymes, but not both simultaneously, can be common. Many bacterial ST systems exhibit autoregulation, with the response regulator (RR) activating the transcription of the operon containing it (Gao and Stock 2013). This too can generate bistability – when the RR level is high, RR gene expression remains high because of the positive feedback loop; but when the RR level is low, the concentration remains at the basal level of expression (Ferrell 2002; Igoshin et al. 2008; Hermsen et al. 2011; Ram and Goulian 2013).

Adaptive fine-tuning vs. inadvertent by-products of pathway structure. Taken together, these theoretical results indicate that without any direct selection at all, the basic structure of ST systems confers the potential for genotypically uniform populations of cells to develop bistability. As described below, this is reflected in a number of dramatic dimorphisms in cell morphology and/or behavior that are almost certainly molded by natural selection. However, there are likely many less visible, molecular-level shifts that may be inadvertent consequences of the structural underpinnings of ST systems.

This being said, while conducive to bistability, feedback-containing networks do not guarantee it (Cherry and Adler 2000; Angeli et al. 2004; Nichol et al. 2016). The actual existence of dual equilibria and the relative sizes of the basins of attraction for the alternative stable points (when they exist) are sensitive to the underlying kinetic parameters of the pathway constituents. For example, changes in the elevation of the activation/deactivation response curve in Figure 22.8b can lead to there being just a single intersection, implying monostability. This then suggests the feasibility of the evolutionary fine-tuning of underlying features of ST systems via the selection of appropriate mutations to favor phenotypic switching vs. uniformity. Indeed, because bistability may often be deleterious, with one or both cellular states far from optimal, selection may often operate to move the key kinetic parameters of ST systems to levels that minimize the chances of phase shifting (Hermsen et al. 2011).

A striking example of the types of processes that govern the dynamics of bistability is known for the bacterium *Bacillus subtilis,* which stochastically switches between a motile single-celled state and a nonmotile, chained state (Norman et al. 2013). Switches to alternative states are governed by a double-negative feedback loop, with each protein suppressing the expression of the other, one conferring the motile, colonizing state and the other promoting biofilm formation. The molecular details can be found in the original paper. The focus here is on the statistical properties of the phase-shifting processes, which are quite different in the two directions.

The motile state is memory-less, in the sense that once initiated, there is a constant probability of switching to the chained state at each subsequent cell division. Letting this probability be p, the probability of switching after the first cell division is p, after the second division is $(1-p)p$, and after the nth division is $(1-p)^n p$. This is an exponential (roughly L-shaped) distribution, with the mean (and standard deviation) of the number of generations to switching both equal to $1/p$, in this case ~ 81 cell divisions. Mechanistically, the stochastic switching appears to be due to rare random fluctuations of the concentrations of proteins underlying the double-negative feedback loop, allowing the previously silenced proteins to escape suppression. Notably, although the distribution of switching times suggests randomness at the population level, the behavior of closely related cells (e.g., sister cells) is correlated, owing to shared effects from the maternal cell (Kaufmann et al. 2007; see Chapter 9).

The distribution of switching times for chains has a very different form, being approximately normal (bell-shaped), with a mean of ~ 8 cell divisions, implying a tight degree of regulation. Here, the underlying molecular mechanism for chain termination is also fairly simple – upon chain initiation, there is a substantial pulse of production of matrix material involved in cell adhesion, which is then diluted over subsequent divisions until a minimum threshold is reached. Taken together, these

results illustrate remarkably simple molecular bases for accomplishing dramatic developmental changes – stochastic molecular switches influencing alternative master regulators for flagellar production and cell adhesion.

One of the key evolutionary questions concerning the dynamics of switching behavior concerns the relative longevities of the alternative phase states and the degree to which natural selection molds them in relationship to the scale of temporal variation in environmental conditions favoring the alternative states. The matter has been explored with an experimental evaluation in the yeast *S. cerevisiae* of a system involving two alternative growth states (Acar et al. 2008). Here, strains were engineered to switch between two physiological states that yielded different growth rates in two alternative environments. The strain that rapidly shifted from one state to the other experienced an early advantage whenever the environment shifted, as it more rapidly produced progeny that were adapted in the changed environment. However, as the length of time between environmental shifts was lengthened, the slow-shifting variant gained an advantage, owing to its reduced production of the maladapted type. Although somewhat contrived, these results show that the long-term advantage of phenotypic switching depends on the temporal dynamics of environmental change.

Not surprisingly, a considerable amount of attention has been given to the adaptive exploitation of bistability as a "bet-hedging" strategy enabling individual genotypes to maximize their long-term fitness without resorting to potentially costly mechanisms for short-term physiological adaptation (Kussell and Leibler 2005; Smits et al. 2006; Veening et al. 2008; Wei et al. 2014; Norman et al. 2015). For reasons of tractability, most of the theoretical work has focused on simple systems with just two discrete environments, each lasting for a time period in excess of cell generation lengths, and with two discrete phenotypes, each better adapted to an alternative environment.

In a temporally variable environment, the genotype with the highest long-term exponential growth rate will be favored, and for the simple two-state / two-environment model, the optimal random phenotypic switching time is equal to the average of the rates of shifts between the two environmental states, provided there are equally large (but opposite in sign) selective pressures on the two alternative phenotypes in the alternative environments (Thattai and van Oudenaarden 2004; Kussell et al. 2005; Salathé et al. 2009; Gaál et al. 2010). On the other hand, if the selection differentials in the two environments are substantially different, stochastic switching can be disfavored, as the monomorphic genotype favored in the environment with large effects can overwhelm the smaller, short-lived disadvantage in the opposite environment. Most environmental variables are continuous in nature, and can vary on both within- and between-generation time scales, as well as spatially, and these kinds of scenarios can lead to rather different expectations (Lynch and Gabriel 1987). Thus, it appears risky to assume that all instances of phenotypic polymorphisms reflect adaptive fine-tuning.

Finally, in all of the preceding discussion, it is assumed that phenotypic switching is an intrinsic feature of a cellular network, occurring without regard to the current environmental state. However, using environmental cues, organisms can, in principle, reinforce various phenotypic outcomes. This might happen, for example, through appropriate epigenetic modifications such as DNA methylation and histone

modifications if these somehow encouraged individuals expressing a particular phenotype to produce offspring with an elevated frequency of the same phenotype (Xue and Leibler 2016). Provided that the individuals with inappropriate phenotypes are removed by selection, so that they too aren't reinforced, such a system can then lead to a form of transgenerational acclimation that superficially appears like learning or the inheritance of acquired characteristics – a transient shift in mean phenotype without any underlying genetic change, which will resort back to an alternative phenotype distribution upon environmental change (see Foundations 9.5).

Summary

- Organisms respond to external environmental stimuli through the use of signal-transduction (ST) pathways that relay information from the cell surface to ultimate effectors, such as transcription-factor binding sites. In most species, dozens to hundreds of such systems are specialized to different environmental indicators. The vast majority of such systems operate via additions and removals of phosphoryl groups on the participating proteins, generally causing switch-like changes in protein structure and function. In bacteria, such information relay systems generally involve just two proteins – an external sensor and a response regulator, whereas more complex, multi-step relay systems, often with multiple intersecting partners, are the rule in eukaryotes.

- ST systems are modular in nature, being based on several several small motifs, typically < 6 amino-acid residues in length, that specify proper communication between sensor and regulator proteins to the exclusion of members of other parallel pathways. Sensor and regulatory proteins are often dimers, requiring specialized motifs for self-assembly and avoidance of heterodimerization. Owing to the simplicity of these communication systems, rewiring of ST pathways is readily accomplished by changes in just a few key amino acids. Although this opens up opportunities for the establishment of novel signaling pathways by gene duplication, it also promotes the neutral drift of the recognition vocabulary in the absence of selection for altered functions.

- Despite the fact that the proteins driving ST systems operate as conventional Michaelis-Menten enzymes, the pathways are often structured in such a way as to potentially generate very steep responses to external ligand concentrations, in some cases approaching ultrasensitivity wherein the downstream target is essentially 100% on or off when the ligand concentration is above or below the threshold value.

- The constant operation of opposing phosphorylation/dephosphorylation reactions at the heart of ST systems imposes a substantial energetic cost of processing and transmitting information, even in a constant environment.

- Owing to fluctuations in the arrival and binding of external signals to cell-surface receptors, environmental sensing is an inherently noisy process. Noise buffering is facilitated by increasing the numbers of receptors and setting the binding kinetics to levels that allow the cell to repeatedly make independent measures of the degree of receptor binding at a rate that exceeds the internal cellular response.

- Eukaryotic ST systems tend to be much more complicated than those in bacteria, with kinases and phosphatases commonly cross-talking with multiple interacting partners, expansions to cascades of multiple intermediate steps, and use of multiple phosphosites per molecule in communication. Many aspects of this complexity do not appear to enhance the efficiency and accuracy of environmental assessment, and it remains an open question as to whether they have been driven by adaptive forces.

- Chemotaxis provides a rapid mechanism for adjusting the direction of bacterial motility through temporal surveys of the environment. These systems, which vary in structure among species, also often have a simple built-in feedback mechanism for adjusting sensitivity to the prevailing environmental state, much like the visual systems of metazoans adjust to different light levels.

- The structure of ST systems is such that the addition of positive feedback loops (or pairs of negative feedbacks) can give rise to bistable responses to external ligand concentrations. By this means, genetically uniform populations can generate dimorphic populations of cells, potentially enhancing long-term genotypic fitness in environments presenting certain levels of variation.

Foundations 22.1. Behavior of a monocycling system. A key issue with respect to an interconvertible enzyme (I) is the degree of activity expected under various conditions. The total concentration of the enzyme $[I_T]$ partitions into the subsets of active and inactive molecules, $[I_a]$ and $[I_i]$, to a degree that depends on the relative concentrations of the active forms of converter enzymes (denoted F and R, respectively, for forward and reverse reactions). The fractional activities of the converter enzymes depend in turn on the concentrations of their ligands and their affinities for them. Because the two converter enzymes push the interconvertible enzyme in opposite directions, the relative concentrations of their active forms dictate the level of activity of enzyme I.

Here we consider the steady-state situation in which the concentrations of both converter enzymes and their ligands are kept constant by ambient cellular conditions. Initially, we further assume that the fractions of both converter enzymes tied up with the interconvertible enzyme are negligible, which requires that the latter not be at a saturating level. Under these conditions (first-order rate kinetics), the activated fractions of both converting enzymes will reach equilibrium levels independent of the amount of enzyme I, and determined only by the rates of association and dissociation with their ligands. Using the terms in Figure 22.4, for the forward enzyme, equilibrium requires that the rate of production of the active (a) enzyme from inactive (i) enzyme equals the flux in the opposite direction (resulting from the deactivation of F_a),

$$k_{a,F}[F_i][S_F] = k_{d,F}[F_a]. \tag{22.1.1}$$

Noting that the total concentration of forward enzyme in the system is

$$[F_T] = [F_i] + [F_a], \tag{22.1.2}$$

solving these two equations leads to the equilibrium concentration of the active forward enzyme

$$[F_a] = \frac{[F_T][S_F]}{k_{D,F} + [S_F]}, \tag{22.1.3a}$$

where $k_{D,F} = k_{d,F}/k_{a,F}$ is the dissociation constant of enzyme F. Likewise, the equilibrium concentration of the active form of the reverse enzyme is

$$[R_a] = \frac{[R_T][S_R]}{k_{D,R} + [S_R]}. \tag{22.1.3b}$$

Provided the concentrations of the converter enzymes are at steady state, the alternative forms of the central enzyme I will also attain equilibrium. This occurs when the rate of production of active from inactive I equals the rate in the opposite direction. Using the familiar Michaelis-Menten formulations (Chapter 19), these forward and reverse reaction rates can be written as

$$V_F = \frac{k_{cat,F}[F_a][I_i]}{k_{S,F} + [I_i]}, \tag{22.1.4a}$$

and

$$V_R = \frac{k_{cat,R}[R_a][I_a]}{k_{S,R} + [I_a]}. \tag{22.1.4b}$$

Letting the total concentration of interconvertible enzyme in the system be

$$[I_T] = [I_i] + [I_a], \tag{22.1.5a}$$

the quantity of interest is the fraction of molecules that are in the active state,

$$\mathrm{I}^* = [\mathrm{I_a}]/[\mathrm{I_T}]. \tag{22.1.5b}$$

The general solution can be obtained by setting Equations 22.1.4a,b equal to each other, letting $[\mathrm{I_i}] = [\mathrm{I_T}] - [\mathrm{I_a}]$, and solving for the level of $[\mathrm{I_a}]$ that satisfies the equality.

As pointed out by Stadtman and Chock (1977), provided the total amount of enzyme I in the system is small relative to the half-saturation constants in Equations 22.1.4a,b (nonsaturating conditions), the concentrations of I in the denominators of these equations can be ignored, and this leads to an expression of the form

$$\mathrm{I}^* = \frac{\beta C}{1 + \beta C}, \tag{22.1.6}$$

where

$$\beta = \frac{\kappa_\mathrm{F}[\mathrm{F_T}]}{\kappa_\mathrm{R}[\mathrm{R_T}]} \tag{22.1.7a}$$

with $\kappa_\mathrm{x} = k_{\mathrm{cat,x}}/k_{\mathrm{S,x}}$, the specificity constant of enzyme x (see Foundations 19.1), being the ratio of kinetic potentials of the forward and reverse converter enzymes, and

$$C = \frac{[S_\mathrm{F}](k_{\mathrm{D,R}} + [S_\mathrm{R}])}{[S_\mathrm{R}](k_{\mathrm{D,F}} + [S_\mathrm{F}])} \tag{22.1.7b}$$

being the ratio of degrees of saturation of the input reactions. Although Equation 22.1.6 has a simple hyperbolic form, the underlying function is quite complex, as it actually depends on ten different parameters (two each of the k_{cat}, k_S, and k_D terms, and the concentrations of the two converter enzymes and their input ligands). Equation 22.3 in the main text gives an expression equivalent to Equation 22.16 in terms of the active concentrations of the forward and reverse enzymes.

There are several significant points with respect to Equation 22.1.6. First, for this case of low overall concentration of I, I^* is independent of the total concentration $[\mathrm{I}_T]$. Second, as in the case of simple Michaelis-Menten kinetics, I^* is a hyperbolic function, in this case of C. Although the latter is itself a complex function, inspection shows a hyperbolic relationship with either ligand concentration. Third, although $\mathrm{I}^* \to 1$ as $(\beta C) \to \infty$, because the relative concentrations of active enzymes are limited by the properties of the system (the total enzyme concentrations, total ligand concentrations, and the dissociation constants), there is an upper bound to βC. Thus, the maximum fractional activity of the central enzyme is generally < 1.0.

Finally, a more general expression allowing for any concentration of I was derived by Goldbeter and Koshland (1981). This general solution does depend on $[\mathrm{I_T}]$, bringing the total number of relevant parameters to eleven, but can be written as a function of three composite parameters,

$$\mathrm{I}^* = \frac{(\alpha - 1) - (k^*_\mathrm{F} + \alpha k^*_\mathrm{R}) + \sqrt{[(\alpha - 1) - (k^*_\mathrm{F} + \alpha k^*_\mathrm{R})]^2 + 4\alpha(\alpha - 1)k^*_\mathrm{R}}}{2\alpha}, \tag{22.1.8}$$

where $\alpha = (k_{\mathrm{cat,F}}[\mathrm{F_a}])/(k_{\mathrm{cat,R}}[\mathrm{R_a}])$, $k^*_\mathrm{F} = k_{\mathrm{S,F}}/[\mathrm{I_T}]$, $k^*_\mathrm{R} = k_{\mathrm{S,R}}/[\mathrm{I_T}]$, and $[\mathrm{F_a}]$ and $[\mathrm{R_a}]$ are defined by Equations 22.1.3a,b. Contrary to the limiting situation in which $[\mathrm{I_T}]$ is low, the relationship of I^* is no longer a simple hyperbola, as discussed in the main text.

The features of additional types of systems, including those with inhibitor interactions and with linked (multicyclic) cycles, are explored in Chock and Stadtman (1977), Stadtman and Chock (1977), and Goldbeter and Koshland (1984). Not surprisingly, these exhibit even richer behavior than those noted above. For the case

of bacterial two-component systems, where the kinase often has a dual function as the phosphatase (the reverse converter enzyme in the above scheme), Batchelor and Goulian (2003) and Rowland and Deeds (2014) have developed expressions similar in form to Equation 22.1.8. An excellent overview of all of these models, and the logic underlying them, is provided by Qian (2007).

Foundations 22.2. Accuracy of environmental sensing. A successful sensing system requires that the information receptors of a must be capable of accurately assaying the current environmental state so that a reliable signal can be transmitted to the downstream responders essential for eliciting appropriate changes in cell behavior. Here, we consider the degree to which a single molecular receptor at the cell surface can assess the concentration of a ligand in the surrounding environment. The assumption is that the fractional time during which the receptor is bound to the external ligand (p) provides the best information that the cell can utilize for environmental prediction. At any single point in time, the receptor is either occupied or not, so a single snap-shot assessment provides little information. Over time, however, because ligand molecules also become unbound, the receptor can make repeated assays of the environment, so that the average occupancy during a particular period becomes an estimate of p. We then inquire as to the variation in such estimates around the true environmental value.

As a measure of accuracy, we utilize the coefficient of variation, which is equivalent to the ratio of the standard deviation (σ_x) to the mean (μ_x) of repeated measures of a variable. Because it is easier to work with measures of variance, which is the square of the standard deviation, the derivations to follow will be based on the squared coefficient of variation, σ_x^2/μ_x^2. It is assumed here that on the time scale of environmental assessment, the cell resides in a homogeneous environment in which the ligand concentration (c_0) is constant, so we are obtaining a pure measurement of environmental sensitivity based on the properties of the receptor molecule and its ligand molecule. If the environment is variable within the time-frame of environmental assessment, the variance of ligand concentration would need to be added to the measure of noise derived below. The following derivations are based on the first presentation of the problem by Berg and Purcell (1977) and subsequent refinements by Kaizu et al. (2014). Some uncertainties about the precise nature of the final formulation are addressed in an excellent overview by Aquino et al. (2016).

To describe the temporal behavior of receptor occupancy, consider the stochastic differential equation

$$\frac{d\Gamma_t}{dt} = k_{\text{on}} c_0 (1 - \Gamma_t) - k_{\text{off}} \Gamma_t + \epsilon_t, \tag{22.2.1}$$

where Γ_t denotes the occupancy (0 or 1) of a single receptor at time point t, k_{on} is the rate of ligand binding to an unbound receptor (conditional on the external concentration), k_{off} is the rate of dissociation of a ligand molecule from a bound receptor, and ϵ_t is a stochastic variable with mean zero. By setting the derivative to zero and solving, the equilibrium probability of occupancy is found to be

$$\overline{\Gamma} = p = \frac{k_{\text{on}} c_0}{k_{\text{on}} c_0 + k_{\text{off}}} = \frac{c_0}{c_0 + k_{\text{D}}}, \tag{22.2.2}$$

where $k_{\text{D}} = k_{\text{off}}/k_{\text{on}}$.

Although the cell perceives the environment through the act of ligand binding, the ultimate goal is to obtain an estimate of the ligand concentration (c) that closely approximates the true concentration (c_0). This requires an estimate of the variance among sample estimates of c_0 inferred from the cell's readout Γ. To obtain this, we

start with a general rule from statistics that the variance of a dependent variable is equal to the variance of a causal variable times the squared derivative of the first with respect to the second, which in this case implies,

$$\sigma_\Gamma^2 = (\partial p/\partial c)^2 \cdot \sigma_c^2. \tag{22.2.3}$$

Rearranging and dividing by c_0^2 yields our desired measure of accuracy, the squared coefficient of variation of inferred concentration,

$$\frac{\sigma_c^2}{c_0^2} = \frac{1}{c_0^2} \cdot \frac{\sigma_\Gamma^2}{(\partial p/\partial c)^2}. \tag{22.2.4}$$

From Equation 22.2.2, the partial derivative evaluated at c_0 is

$$\frac{\partial p}{\partial c} = \frac{k_\mathrm{D}}{(c_0 + k_\mathrm{D})^2}, \tag{22.2.5}$$

and substitution into Equation 22.2.4 leads, after some rearrangement, to

$$\frac{\sigma_c^2}{c_0^2} = \frac{c_0^2}{p^4 k_\mathrm{D}^2} \cdot \sigma_\Gamma^2. \tag{22.2.6}$$

The final step requires an expression for the variance in the mean occupancy σ_Γ^2 over some period of time T of continuous assessment, computation of which is complicated by the fact that the realized Γ at any one particular time is not independent of that in adjacent time periods, owing to the time spans between ligand binding and release. Taking these autocorrelations into consideration, Berg and Purcell (1977) showed that

$$\sigma_\Gamma^2 = \frac{2p(1-p)^2}{Tk_\mathrm{off}}. \tag{22.2.7a}$$

Noting from Equation 22.2.2 that

$$k_\mathrm{on} c_0 (1-p) = k_\mathrm{off} p,$$

Equation 22.2.7a can be equivalently written as

$$\sigma_\Gamma^2 = \frac{2p^2(1-p)}{Tk_\mathrm{on}} c_0. \tag{22.2.7b}$$

Finally, substituting Equation 22.2.7b into 22.2.6, again with some downstream rearrangement, leads to a remarkably simple expression

$$\frac{\sigma_c^2}{c_0^2} = \frac{2}{pTk_\mathrm{off}} = \frac{2}{(1-p)Tk_\mathrm{on}c_0}. \tag{22.2.8}$$

The accuracy of assessment increases (i.e., σ_c^2/c_0^2 decreases) with increasing time over which the cell integrates environmental information, and also with increasing k_off. The latter feature arises because the inverse of k_off is equal to the average release time of ligands, which means that higher k_off allows the receptor to make more evaluations of the environment.

There are two other ways to express the accuracy. First, the average time between consecutive ligand-binding events is equal to the sum of the mean times for the length

of binding to an occupied receptor and that of the time for an unoccupied receptor to accept another ligand, each of which is the reciprocal of the respective rate,

$$\tau_b = \frac{1}{k_{\text{off}}} + \frac{1}{k_{\text{on}} c_0}. \tag{22.2.9}$$

Noting that the mean number of expected bindings in interval T is $\overline{N} = T/\tau_b$, substitution of $T = \overline{N}\tau_b$ and Equation 22.2.2 nto 22.2.8 leads to

$$\frac{\sigma_c^2}{c_0^2} = \frac{2}{\overline{N}}, \tag{22.2.10}$$

showing that the squared CV of the cell's estimate of c_0 is inversely proportional to the expected number of molecules bound (which itself is a function of time and ligand concentration).

Second, k_{on} is the inverse of the mean time to binding of an unoccupied receptor, with the latter being equal to the inverse of the sum of expected times for particles to diffuse to the receptor (k_e) and of binding upon contact (k_+),

$$k_{\text{on}} = \left(\frac{1}{k_e} + \frac{1}{k_+}\right)^{-1} = \frac{k_e k_+}{k_e + k_+}. \tag{22.2.11}$$

Assuming the receptor binding site can be approximated as disc of radius s on the cell surface, the encounter rate (per unit concentration) by diffusion is

$$k_e = 4Ds, \tag{22.2.12}$$

where D is the diffusion constant for the ligand. Substituting Equation 22.2.11 into 22.2.8 yields

$$\frac{\sigma_c^2}{c_0^2} = \frac{2}{Tc_0(1-p)}\left(\frac{1}{k_e} + \frac{1}{k_+}\right). \tag{22.2.13a}$$

Berg and Purcell (1977) assumed the case of diffusion limitation, such that $k_e \ll k_+$, which reduces Equation 22.2.13a to

$$\frac{\sigma_c^2}{c_0^2} = \frac{1}{2Dsc_0(1-p)T}. \tag{22.2.13b}$$

To gain more quantitative insight into the accuracy of monitoring as inferred by Equation 22.2.13b, let $D = 10^{-5}$ cm^2/sec, which closely approximates true values for single amino acids (with cations and anions having values only $\sim 2\times$ higher; Chapter 7). Estimates of s for chemoreceptors are sparse, but can be inferred to be on the order of 2 nm ($= 2 \times 10^{-7}$ cm) given that the total area of receptor arrays in a wide range of bacteria implies an area/receptor of ~ 100 nm^2 with most of the array space being empty (Briegel et al. 2009). Supposing the dissociation constant K_D is such that $p \simeq 0.5$ (Equation 22.2.2), and a ligand concentration of $c_0 = 1\,\mu\text{M} = 6 \times 10^{14}$ molecules/cm^3, the coefficient of variation of measurement becomes

$$\frac{\sigma_c}{c_0} = \sqrt{\frac{1}{1000T}}$$

where the units of T are in seconds. Thus, monitoring a constant environment for just ten seconds is sufficient to reduce the level of estimation noise to 0.01 (i.e., a standard deviation of the inferred concentration just 1% of the true value). Assuming the same p, with a 1000-fold lower concentration of 1 nM, the level of uncertainty will be increased by a factor of $\sqrt{1000} \simeq 32$, and to achieve a level of accuracy of 0.01, T has to be 1000-fold higher.

Literature Cited

Abedrabbo, S., J. Castellon, K. D. Collins, K. S. Johnson, and K. M. Ottemann. 2017. Cooperation of two distinct coupling proteins creates chemosensory network connections. Proc. Natl. Acad. Sci. USA 114: 2970-2975.

Acar, M., J. T Mettetal, and A. van Oudenaarden. 2008. Stochastic switching as a survival strategy in fluctuating environments. Nature Genetics 40: 471-475.

Adler, J. 1966. Chemotaxis in bacteria. Science 153: 708-716.

Alm, E., K. Huang, and A. Arkin. 2006. The evolution of two-component systems in bacteria reveals different strategies for niche adaptation. PLoS Comput. Biol. 2: e143.

Anantharaman, V., L. M. Iyer, and L. Aravind. 2007. Comparative genomics of protists: new insights into the evolution of eukaryotic signal transduction and gene regulation. Ann. Rev. Microbiol. 61: 453-475.

Angeli, D., J. E. Ferrell, Jr., and E. D. Sontag. 2004. Detection of multistability, bifurcations, and hysteresis in a large class of biological positive-feedback systems. Proc. Natl. Acad. Sci. USA 101: 1822-1827.

Aquino, G., N. S. Wingreen, and R. G. Endres. 2016. Know the single-receptor sensing limit? Think again. J. Stat. Phys. 162: 1353-1364.

Armbruster, D., J. Nagy, and J. Young. 2014. Three level signal transduction cascades lead to reliably timed switches. J. Theor. Biol. 361: 69-80.

Ashenberg, O., K. Rozen-Gagnon, M. T. Laub, and A. E. Keating. 2011. Determinants of homodimerization specificity in histidine kinases. J. Mol. Biol. 413: 222-235.

Ballal, A., R. Heermann, K. Jung, M. Gassel, K. Apte, and K. Altendorf. 2002. A chimeric *Anabaena / Escherichia coli* KdpD protein (Anacoli KdpD) functionally interacts with *E. coli* KdpE and activates kdp expression in *E. coli.* Arch. Microbiol. 178: 141-148.

Barkai, N., and S. Leibler. 1997. Robustness in simple biochemical networks. Nature 387: 913-917.

Batchelor, E., and M. Goulian. 2003. Robustness and the cycle of phosphorylation and dephosphorylation in a two-component regulatory system. Proc. Natl. Acad. Sci. USA 100: 691-696.

Berg, H. C., and E. M. Purcell. 1977. Physics of chemoreception. Biophys. J. 20: 193-219.

Bitbol, A. F., and N. S. Wingreen. 2015. Fundamental constraints on the abundances of chemotaxis proteins. Biophys. J. 108: 1293-1305.

Blüthgen N. 2006. Sequestration shapes the response of signal transduction cascades. IUBMB Life 58: 659-663.

Briegel, A., et al. 2009. Universal architecture of bacterial chemoreceptor arrays. Proc. Natl. Acad. Sci. USA 106: 17181-17186.

Briegel, A., D. R. Ortega, A. N. Huang, C. M. Oikonomou, R. P. Gunsalus, and G. J. Jensen. 2015. Structural conservation of chemotaxis machinery across Archaea and Bacteria. Environ. Microbiol. Rep. 7: 414-419.

Burger, L., and E. van Nimwegen. 2008. Accurate prediction of protein-protein interactions from sequence alignments using a Bayesian method. Mol. Syst. Biol. 4: 165.

Capra, E. J., and M. T. Laub. 2012. Evolution of two-component signal transduction systems. Annu. Rev. Microbiol. 66: 325-347.

Capra, E. J., B. S. Perchuk, O. Ashenberg, C. A. Seid, H. R. Snow, J. M. Skerker, and M. T. Laub. 2012a. Spatial tethering of kinases to their substrates relaxes evolutionary constraints on specificity. Mol. Microbiol. 86: 1393-1403.

Capra, E. J., B. S. Perchuk, E. A. Lubin, O. Ashenberg, J. M. Skerker, and M. T. Laub. 2010. Systematic dissection and trajectory-scanning mutagenesis of the molecular interface that ensures specificity of two-component signaling pathways. PLoS Genet. 6: e1001220.

Capra, E. J., B. S. Perchuk, J. M. Skerker, and M. T. Laub. 2012b. Adaptive mutations that prevent crosstalk enable the expansion of paralogous signaling protein families. Cell 150: 222-232.

Cherry, J. L., and F. R. Adler. 2000. How to make a biological switch. J. Theor. Biol. 203: 117-133.

Chock, P. B., and E. R. Stadtman. 1977. Superiority of interconvertible enzyme cascades in metabolite regulation: analysis of multicyclic systems. Proc. Natl. Acad. Sci. USA 74: 2766-2770.

Cock, P. J., and D. E. Whitworth. 2007. Evolution of prokaryotic two-component system signaling pathways: gene fusions and fissions. Mol. Biol. Evol. 24: 2355-2357.

Colin, R., and V. Sourjik. 2017. Emergent properties of bacterial chemotaxis pathway. Curr. Opin. Microbiol. 39: 24-33.

Cremer, J., T. Honda, Y. Tang, J. Wong-Ng, M. Vergassola, and T. Hwa. 2019. Chemotaxis as a navigation strategy to boost range expansion. Nature 575: 658-663.

Endres, R. G., and N. S. Wingreen. 2008. Accuracy of direct gradient sensing by single cells. Proc. Natl. Acad. Sci. USA 105: 15749-15754.

Endres, R. G., and N. S. Wingreen. 2009. Maximum likelihood and the single receptor. Phys. Rev. Lett. 103: 158101.

Ferrell, J. E., Jr. 2002. Self-perpetuating states in signal transduction: positive feedback, double-negative feedback and bistability. Curr. Opin. Cell Biol. 14: 140-148.

Gaál, B., J. W. Pitchford, and A. J. Wood. 2010. Exact results for the evolution of stochastic switching in variable asymmetric environments. Genetics 184: 1113-1119.

Gao, R., and A. M. Stock. 2013. Evolutionary tuning of protein expression levels of a positively autoregulated two-component system. PLoS Genet. 9: e1003927.

Gildor, T., R. Shemer, A. Atir-Lande, and D. Kornitzer. 2005. Coevolution of cyclin Pcl5 and its substrate Gcn4. Eukaryot. Cell 4: 310-318.

Goldbeter, A., and D. E. Koshland, Jr. 1981. An amplified sensitivity arising from covalent modification in biological systems. Proc. Natl. Acad. Sci. USA 78: 6840-6844.

Goldbeter, A., and D. E. Koshland, Jr. 1984. Ultrasensitivity in biochemical systems controlled by covalent modification: interplay between zero-order and multistep effects. J. Biol. Chem. 259: 14441-14447.

Goldbeter, A., and D. E. Koshland, Jr. 1987. Energy expenditure in the control of biochemical

systems by covalent modification. J. Biol. Chem. 262: 4460-4471.

Goulian, M. 2010. Two-component signaling circuit structure and properties. Curr. Opin. Microbiol. 13: 184-189.

Govern, C. C., and P. R. Ten Wolde. 2014. Optimal resource allocation in cellular sensing systems. Proc. Natl. Acad. Sci. USA 111: 17486-17491.

Gunawardena, J. 2005. Multisite protein phosphorylation makes a good threshold but can be a poor switch. Proc. Natl. Acad. Sci. USA 102: 14617-14622.

Hansen, J., E. Mailand, K. K. Swaminathan, J. Schreiber, B. Angelici, and Y. Benenson. 2014. Transplantation of prokaryotic two-component signaling pathways into mammalian cells. Proc. Natl. Acad. Sci. USA 111: 15705-15710.

Hermsen, R., D. W. Erickson, and T. Hwa. 2011. Speed, sensitivity, and bistability in auto-activating signaling circuits. PLoS Comput. Biol. 7: e1002265.

Igoshin, O. A., R. Alves, and M. A. Savageau. 2008. Hysteretic and graded responses in bacterial two-component signal transduction. Mol. Microbiol. 68: 1196-1215.

Iyengar, G., M. and Rao. 2014. A cellular solution to an information-processing problem. Proc. Natl. Acad. Sci. USA 111: 12402-1247.

Kaizu, K., W. de Ronde, J. Paijmans, K. Takahashi, F. Tostevin, and P. R. ten Wolde. 2014. The Berg-Purcell limit revisited. Biophys. J. 106: 976-985.

Kaufmann, B. B., Q. Yang, J. T. Mettetal, and A. van Oudenaarden. 2007. Heritable stochastic switching revealed by single-cell genealogy. PLoS Biol. 5: e239.

Keymer, J. E., R. G. Endres, M. Skoge, Y. Meir, and N. S. Wingreen. 2006. Chemosensing in *Escherichia coli:* two regimes of two-state receptors. Proc. Natl. Acad. Sci. USA 103: 1786-1791.

Koretke, K. K., A. N. Lupas, P. V. Warren, M. Rosenberg, and J. R. Brown. 2000. Evolution of two-component signal transduction. Mol. Biol. Evol. 17: 1956-1970.

Kussell, E., R. Kishony, N. Q. Balaban, and S. Leibler. 2005. Bacterial persistence: a model of survival in changing environments. Genetics 169: 1807-1814.

Kussell, E., and S. Leibler. 2005. Phenotypic diversity, population growth, and information in fluctuating environments. Science 309: 2075-2078.

Lan, G., P. Sartori, S. Neumann, V. Sourjik, and Y. Tu. 2012. The energy-speed-accuracy tradeoff in sensory adaptation. Nat. Physics 8: 422-428.

Landauer, R. 1988. Dissipation and noise immunity in computation and communication. Nature 335: 779-784.

Laub, M. T., and M. Goulian. 2007. Specificity in two-component signal transduction pathways. Annu. Rev. Genet. 41: 121-145.

Li, L., E. I. Shakhnovich, and L. A. Mirny. 2003. Amino acids determining enzyme-substrate specificity in prokaryotic and eukaryotic protein kinases. Proc. Natl. Acad. Sci. USA 100: 4463-4468.

Lim, W., B. Mayer, and T. Pawson. 2014. Cell Signaling. Garland Science, New York, NY.

Loomis, W. F., G. Shaulsky, and N. Wang. 1997. Histidine kinases in signal transduction pathways of eukaryotes. J. Cell Sci. 110: 1141-1145.

Lynch, M., and W. Gabriel. 1987. Environmental tolerance. American Naturalist 129: 283-303.

Lynch, M., and K. Hagner. 2014. Evolutionary meandering of intermolecular interactions along the drift barrier. Proc. Natl. Acad. Sci. USA 112: E30-E38.

Lynch, M., and J. B. Walsh. 1998. Genetics and Analysis of Quantitative Traits. Sinauer Assocs., Inc., Sunderland, MA.

Makarova, K. S., M. Y. Galperin, and E. V. Koonin. 2017. Proposed role for KaiC-like ATPases as major signal transduction hubs in Archaea. mBio 8: e01959-17.

McClune, C. J., A. Alvarez-Buylla, C. A. Voigt, and M. T. Laub. 2019. Engineering orthogonal signalling pathways reveals the sparse occupancy of sequence space. Nature 574: 702-706.

Mello, B. A., L. Shaw, and Tu Y. 2004. Effects of receptor interaction in bacterial chemotaxis. Biophys. J. 87: 1578-1595.

Mello, B. A., and Y. Tu. 2007. Effects of adaptation in maintaining high sensitivity over a wide range of backgrounds for *Escherichia coli* chemotaxis. Biophys. J. 92: 2329-2337.

Mehta, P., and D. J. Schwab. 2012. Energetic costs of cellular computation. Proc. Natl. Acad. Sci. USA 109: 17978-17982.

Ni, B., R. Colin, H. Link, R. G. Endres, and V. Sourjik. 2020. Growth-rate dependent resource investment in bacterial motile behavior quantitatively follows potential benefit of chemotaxis. Proc. Natl. Acad. Sci. USA 117: 595-601.

Nichol, D., M. Robertson-Tessi, P. Jeavons, and A. R. Anderson. 2016. Stochasticity in the genotype-phenotype map: implications for the robustness and persistence of bet-hedging. Genetics 204: 1523-1539.

Niven, J. E. 2016. Neuronal energy consumption: biophysics, efficiency and evolution. Curr. Opin. Neurobiol. 41: 129-135.

Norman, T. M., N. D. Lord, J. Paulsson, and R. Losick. 2013. Memory and modularity in cell-fate decision making. Nature 503: 481-486.

Norman, T. M., N. D. Lord, J. Paulsson, and R. Losick. 2015. Stochastic switching of cell fate in microbes. Annu. Rev. Microbiol. 69: 381-403.

Ortega, F., L. Acerenza, H. V. Westerhoff, F. Mas, and M. Cascante. 2002. Product dependence and bifunctionality compromise the ultrasensitivity of signal transduction cascades. Proc. Natl. Acad. Sci. USA 99: 1170-1175.

Podgornaia, A. I., and M. T. Laub. 2015. Pervasive degeneracy and epistasis in a protein-protein interface. Science 347: 673-677.

Porter, S. L., and J. P. Armitage. 2002. Phosphotransfer in *Rhodobacter sphaeroides* chemotaxis. J. Mol. Biol. 324: 35-45.

Porter, S. L., and J. P. Armitage. 2004. Chemotaxis in *Rhodobacter sphaeroides* requires an atypical histidine protein kinase. J. Biol. Chem. 279: 54573-54580.

Qian, H. 2007. Phosphorylation energy hypothesis: open chemical systems and their biological functions. Annu. Rev. Phys. Chem. 58: 113-142.

Ram, S., and M. Goulian. 2013. The architecture of a prototypical bacterial signaling circuit enables a single point mutation to confer novel network properties. PLoS Genet. 9: e1003706.

Rowland, M. A., and E. J. Deeds. 2014. Crosstalk and the evolution of specificity in two-component signaling. Proc. Natl. Acad. Sci. USA 111: 5550-5555.

Rowland, M. A, W. Fontana, and E. J. Deeds. 2012. Crosstalk and competition in signaling networks. Biophys. J. 103: 2389-2398.

Salathé, M., J. Van Cleve, and M. W. Feldman. 2009. Evolution of stochastic switching rates in asymmetric fitness landscapes. Genetics 182: 1159-1164.

Schaller, G. E., S. H. Shiu, and J. P. Armitage. 2011. Two-component systems and their co-option for eukaryotic signal transduction. Curr. Biol. 21: R320-R330.

Shacter, E., P. B. Chock, and E. R. Stadtman. 1984. Energy consumption in a cyclic phosphorylation/dephosphorylation cascade. J. Biol. Chem. 259: 12260-12264.

Shi, L., N. Pigeonneau, V. Ravikumar, P. Dobrinic, B. Macek, D. Franjevic, M.-F. Noirot-Gros, and I. Mijakovic. 2014. Cross-phosphorylation of bacterial serine/threonine and tyrosine protein kinases on key regulatory residues. Front. Microbiol. 5: 495.

Siryaporn, A., and M. Goulian. 2008. Cross-talk suppression between the CpxA-CpxR and EnvZ-OmpR two-component systems in *E. coli*. Mol. Microbiol. 70: 494-506.

Siryaporn, A., B. S. Perchuk, M. T. Laub, and M. Goulian. 2010. Evolving a robust signal transduction pathway from weak cross-talk. Mol. Syst. Biol. 6: 452.

Skerker, J. M., B. S. Perchuk, A. Siryaporn, E. A. Lubin, O. Ashenberg, M. Goulian, and M. T. Laub. 2008. Rewiring the specificity of two-component signal transduction systems. Cell 133: 1043-1054.

Skoge, M., H. Yue, M. Erickstad, A. Bae, H. Levine, A. Groisman, W. F. Loomis, and W. J. Rappel. 2014. Cellular memory in eukaryotic chemotaxis. Proc. Natl. Acad. Sci. USA 111: 14448-144453.

Smits, W. K., O. P. Kuipers, and J. W. Veening. 2006. Phenotypic variation in bacteria: the role of feedback regulation. Nat. Rev. Microbiol. 4: 259-271.

Sonenshein, A. L. 2000. Control of sporulation initiation in *Bacillus subtilis.* Curr. Opin. Microbiol. 3: 561-566.

Stadtman, E. R., and P. B. Chock. 1977. Superiority of interconvertible enzyme cascades in metabolic regulation: analysis of monocyclic systems. Proc. Natl. Acad. Sci. USA 74: 2761-2765.

Stock, A. M., V. L. Robinson, and P. N. Goudreau. 2000. Two-component signal transduction. Annu. Rev. Biochem. 69: 183-215.

Szurmant, H., T. J. Muff, and G. W. Ordal. 2004. *Bacillus subtilis* CheC and FliY are members of a novel class of CheY-P-hydrolyzing proteins in the chemotactic signal transduction cascade. J. Biol. Chem. 279: 21787-21792.

Tabatabai N, Forst S. 1995. Molecular analysis of the two-component genes, *ompR* and *envZ,* in the symbiotic bacterium *Xenorhabdus nematophilus.* Mol. Microbiol. 17: 643-652.

Taylor, T. B., G. Mulley, A. H. Dills, A. S. Alsohim, L. J. McGuffin, D. J. Studholme, M. W. Silby, M. A. Brockhurst, L. J. Johnson, and R. W. Jackson. 2015. Evolutionary resurrection of flagellar motility via rewiring of the nitrogen regulation system. Science 347: 1014-1107.

Thattai, M., and A. van Oudenaarden. 2004. Stochastic gene expression in fluctuating environments. Genetics 167: 523-530.

Ulrich, L. E., E. V. Koonin, and I. B. Zhulin. 2005. One-component systems dominate signal transduction in prokaryotes. Trends Microbiol. 13: 52-56.

van Haastert, P. J., and M. Postma. 2007. Biased random walk by stochastic fluctuations of chemoattractant-receptor interactions at the lower limit of detection. Biophys. J. 93: 1787-1796.

Veening, J. W., W. K. Smits, and O. P. Kuipers. 2008. Bistability, epigenetics, and bet-hedging in bacteria. Annu. Rev. Microbiol. 62: 193-210.

Wadhams, G. H., A. C. Martin, A. V. Warren, and J. P. Armitage. 2005. Requirements for chemotaxis protein localization in *Rhodobacter sphaeroides*. Mol. Microbiol. 58: 895-902.

Wegener-Feldbrügge, S., and L. Søgaard-Andersen. 2009. The atypical hybrid histidine protein kinase RodK in *Myxococcus xanthus:* spatial proximity supersedes kinetic preference in phosphotransfer reactions. J. Bacteriol. 191: 1765-1776.

Wei, K., M. Moinat, T. R. Maarleveld, and F. J. Bruggeman. 2014. Stochastic simulation of prokaryotic two-component signalling indicates stochasticity-induced active-state locking and growth-rate dependent bistability. Mol. Biosyst. 10: 2338-2346.

Weigt, M., R. A. White, H. Szurmant, J. A. Hoch, and T. Hwa. 2009. Identification of direct residue contacts in protein-protein interaction by message passing. Proc. Natl. Acad. Sci. USA 106: 67-72.

Wuichet, K., B. J. Cantwell, and I. B. Zhulin. 2010. Evolution and phyletic distribution of two-component signal transduction systems. Curr. Opin. Microbiol. 13: 219-225.

Xu, Y., and J. Gunawardena. 2012. Realistic enzymology for post-translational modification: zero-order ultrasensitivity revisited. J. Theor. Biol. 311: 139-152.

Xue, B., and S. Leibler. 2016. Evolutionary learning of adaptation to varying environments through a transgenerational feedback. Proc. Natl. Acad. Sci. USA 113: 11266-11271.

Yamamoto, K., K. Hirao, T. Oshima, H. Aiba, R. Utsumi, and A. Ishihama. 2005. Functional characterization in vitro of all two-component signal transduction systems from *Escherichia coli*. J. Biol. Chem. 280: 1448-1456.

Yang, Y., A. Pollard, C. Höfler, G. Poschet, M. Wirtz, R. Hell, and V. Sourjik. 2015. Relation between chemotaxis and consumption of amino acids in bacteria. Mol. Microbiol. 96: 1272-1282.

Zarrinpar, A., S. H. Park, and W. A. Lim. 2003. Optimization of specificity in a cellular protein interaction network by negative selection. Nature 426: 676-680.

Zhang, W., and L. Shi. 2005. Distribution and evolution of multiple-step phosphorelay in prokaryotes: lateral domain recruitment involved in the formation of hybrid-type histidine kinases. Microbiology 151: 2159-2173.

Figure 22.1. Idealized schematics for bacterial one-component, two-component, and phospho-relay systems for signal transduction. Different colored ovals denote protein domains (contained within the same protein if connected by a black line). Double lines denote cellular membranes. For the latter two systems, the covalently attached phosphate (P) group is derived from ATP subsequent to receipt of an external signal. Phospho-relays can have more complex structures than the one illustrated, with the first P transfer sometimes being to a separate protein, and with multiple players involved in longer chains of reaction.

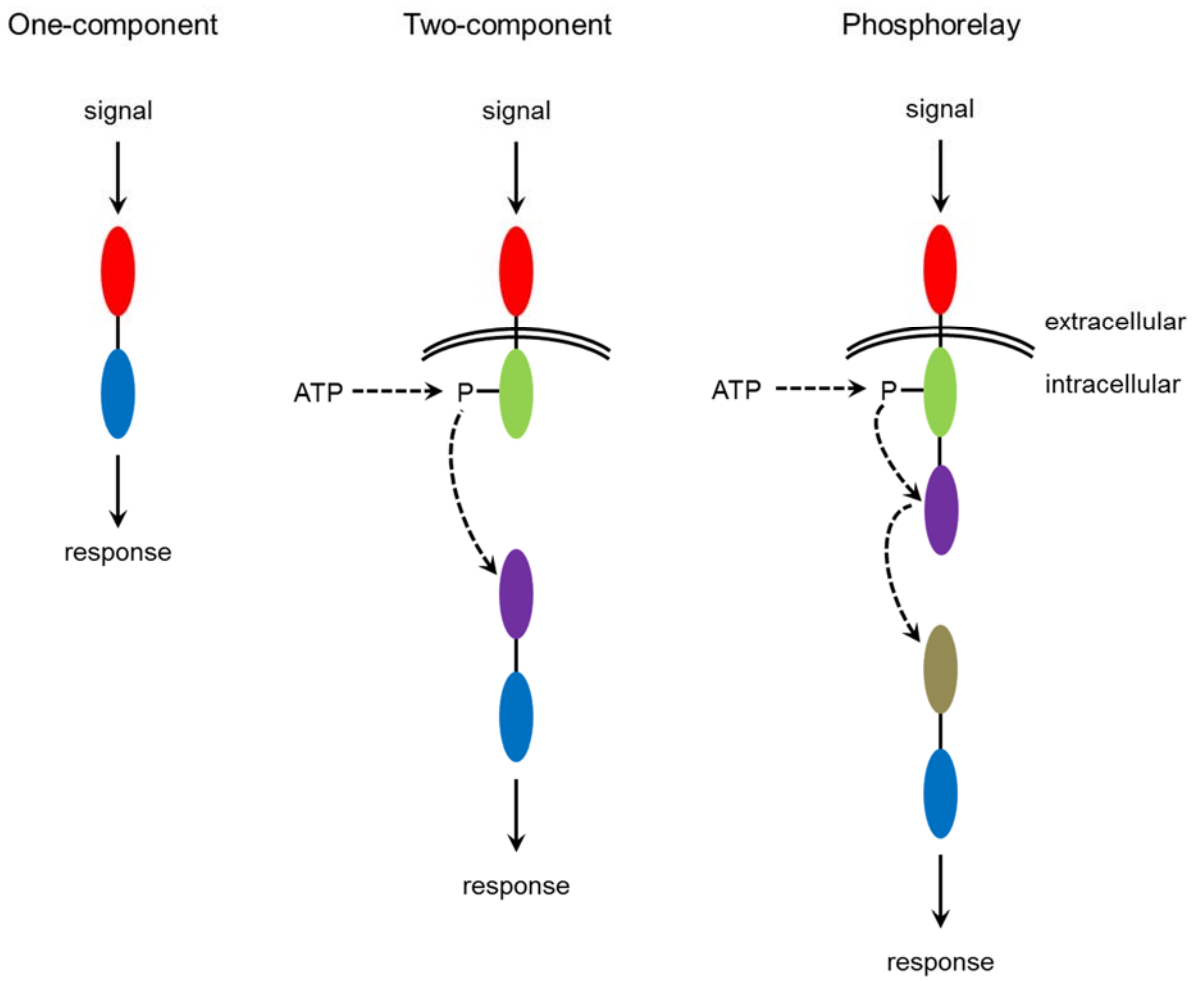

Figure 22.2. Scaling of the number of response regulator (RR) and histidine kinases (HK) proteins involved in two-component systems, and of the number of such systems with total genome size, in a wide range of bacterial species. The diagonal lines denote the range of conditions in which HK proteins are 1 to 2× as abundant as RR proteins. From Capra and Laub (2012).

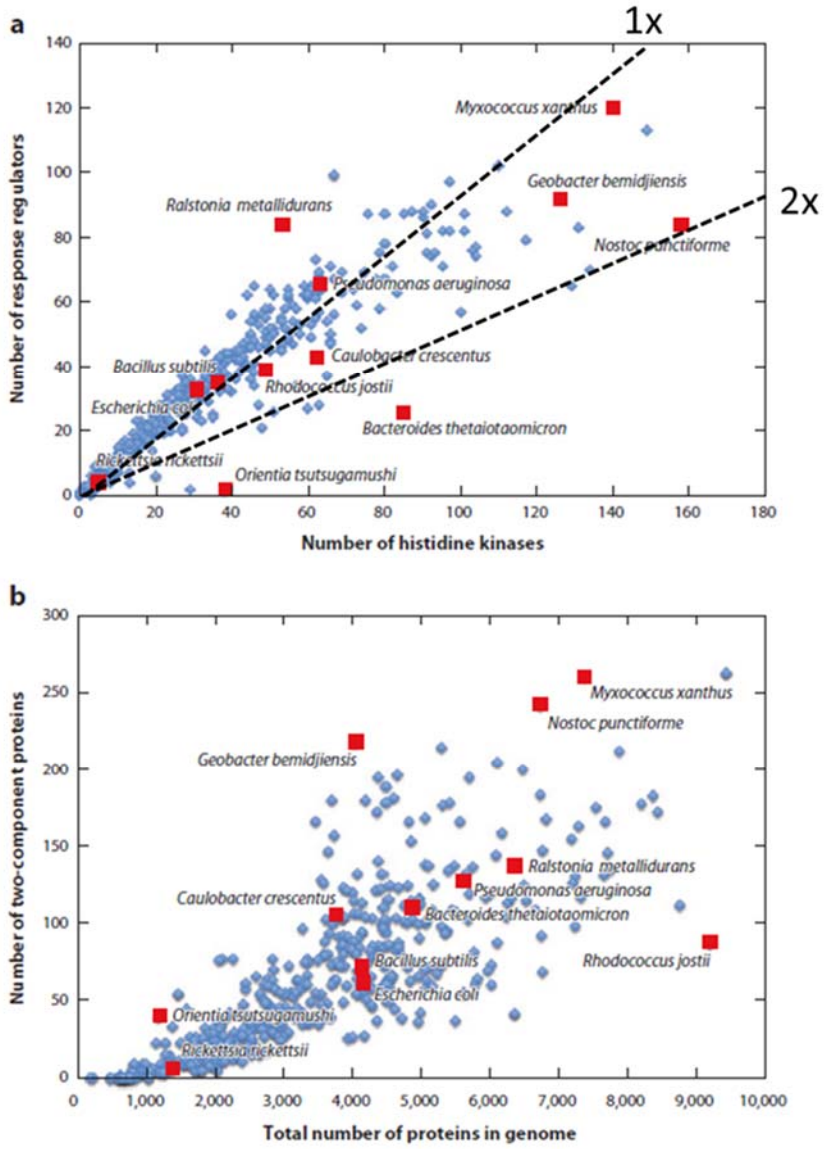

Figure 22.3. A general schematic for what might be necessary for the preservation and long-term divergence of a duplicated HK-RR pair. For the particular scenario noted, one system diverges and the other remains the same, it is not necessary, and perhaps not even likely, that only one pair would undergo functionally significant evolutionary changes. If the two systems are to evolve to be completely insulated from each other, new dimerization domains need to emerge for both the HK and RR proteins, and a new feature of the phosphoryl transfer mechanism would need to be incorporated. Open and closed black dots denote two types of signaling ligands in the extracellular environment. The red and green ovals denote domains of the membrane-bound HK proteins, red being the sensory domain, and green being the autophosphorylation domain. Purple and blue ovals denote domains of the intracellular RR proteins, purple denoting the phosphotransfer domain, and blue denoting the DNA binding (or other output) domain. Open vs. closed ovals and solid vs. dashed lines denote functional changes, with the system on the right no longer capable of crosstalk with the system on the left.

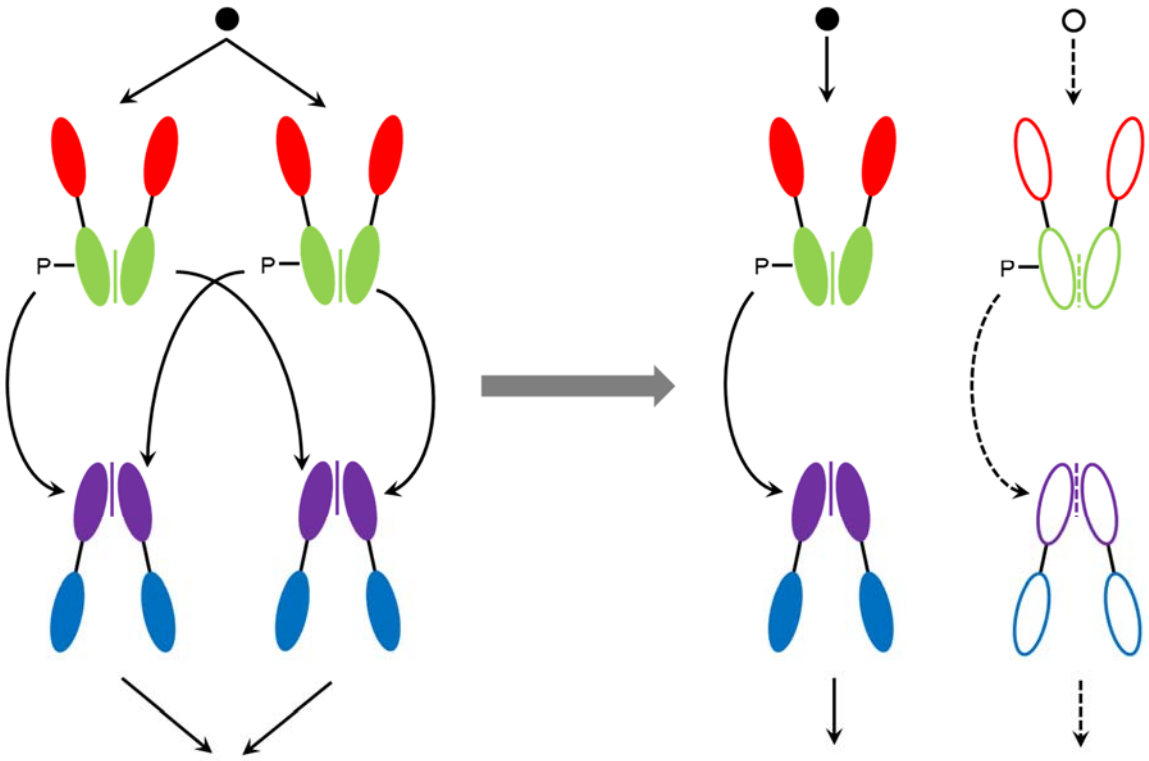

Figure 22.4. Left) Generalized scheme for a monocyclic cascade. An interconvertible protein I is transformed between active (a) and inactive (i) states by forward- (F) and reverse-acting (R) enzymes, which themselves have active and inactive forms dependent on their respective ligands, S_{F} and S_{R}. The k coefficients denote the association (a) and dissociation (d) constants between the ligands and the converting enzymes. **Right)** The reaction equations involving the interconvertible enzymes, with Pi denoting inorganic phosphate.

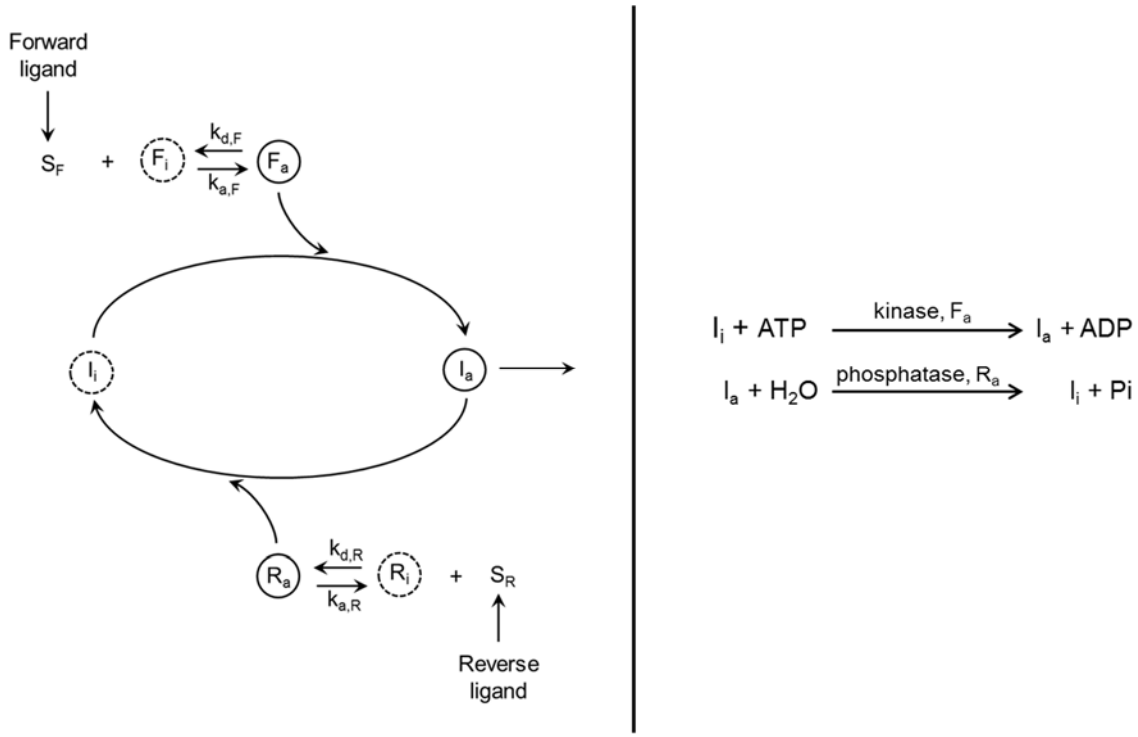

Figure 22.5. Response of the active fraction of an interconvertible protein (I^*) to the concentration of ligand for the forward converting enzyme, $[S_F]$. Both plots are derived using Equation 22.1.8, with the upper curve denoting the limiting behavior when the concentration of I is well below the half-saturation constants of the converting enzymes, Equation 22.1.6. **Upper panel)** Results are given for the situation in which the concentration of the ligand for the reverse enzyme, $[S_R]$, is set equal to 1.0, with increasing levels of $[S_F]$ (according to Equation 22.1.6, the results depend only on the ratio of these two concentrations). The dissociation constant for the forward enzyme and its ligand (equivalent to its half-saturation constant) is $k_{D,F} = 1.0$, with results given for different values of $k_{D,R}$. The parameter β is the ratio of kinetic potentials of the forward and reverse converter enzymes, as defined in Foundations 22.2. As β and $k_{D,R}$ increase, autophosphorylation increasingly dominates and the response curves shift to the left. The black dotted line denotes the situation that would be expected if the response followed the Michaelis-Menten enzyme kinetics of the forward converter and its ligand. **Bottom panel)** Results are given for increasing total concentrations of the interconvertible enzyme. Both of the ligand concentrations and all of the catalytic coefficients and half-saturation constants are arbitrarily set to 1.0.

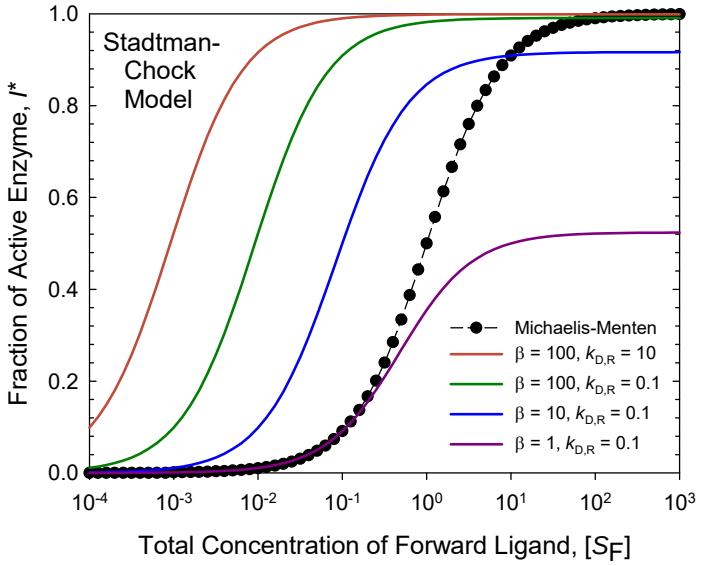

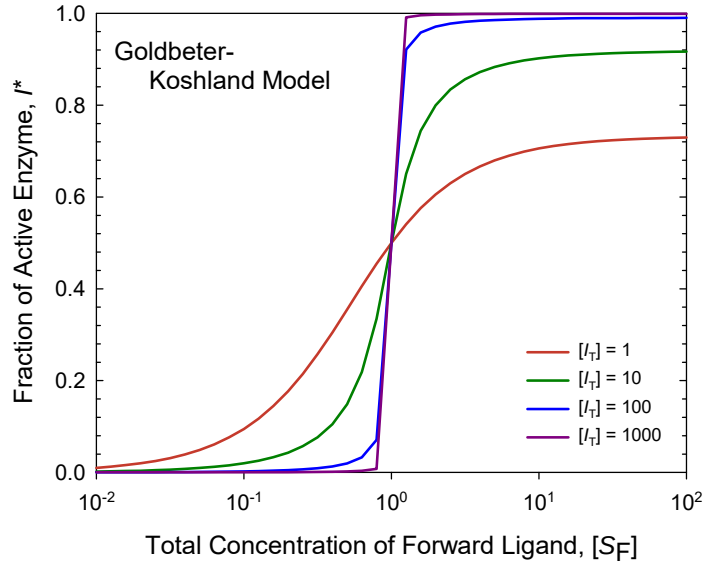

Figure 22.6. Three variants on the structure of signal-transduction pathways commonly found in eukaryotes, with notation as in Figure 22.4.

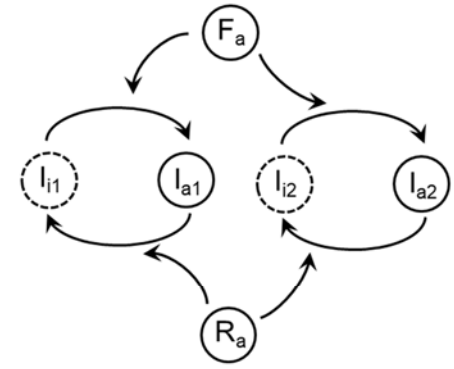

A kinase and a phosphatase sharing two intermediate substrates

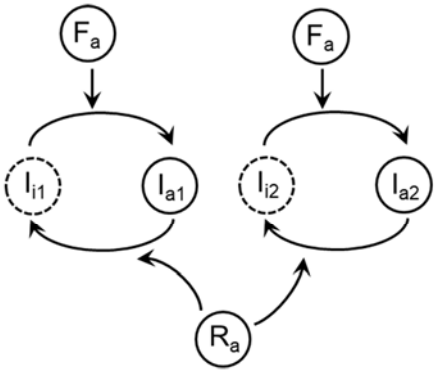

Two independently acting kinases, with one shared phosphatase

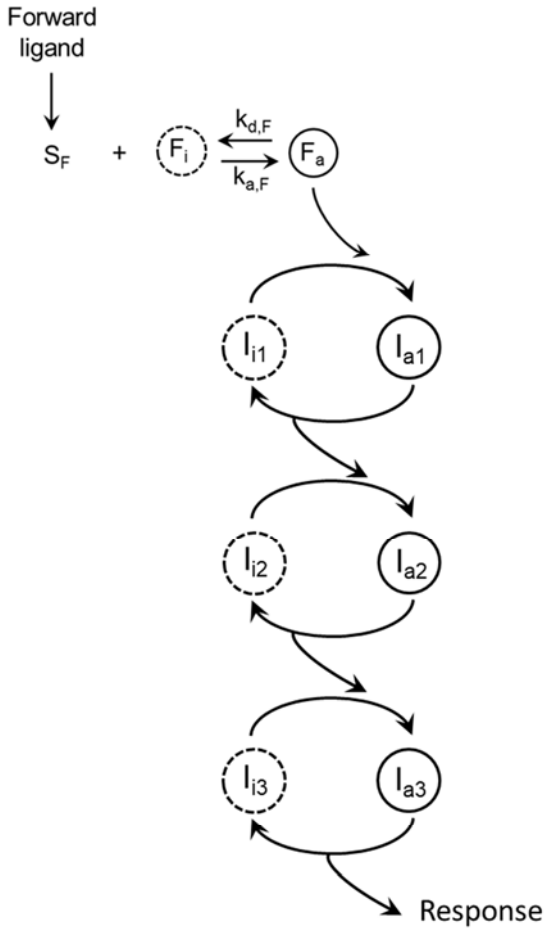

Triple cascade

Figure 22.7. Idealized schematic of the chemotaxis pathway in *E. coli*. The histidine kinase CheA is linked to the external sensors by another protein called CheW. In the absence of ligand binding, CheA becomes phosphorylated, thereby phosphorylating CheY, which binds to the base of the flagellum inducing clockwise rotation and random tumbling. In the presence of ligand (red dots) binding and dephosphorylation of CheY, the flagellum rotates in a counter-clockwise fashion, causing the cell to propel forward in a directed manner. Proteins not specifically mentioned in the text: CheZ is a phosphatase that acts on CheY-P; CheR and CheB are methylases and demethylases that operate on the MCP sensory proteins (dark circles and ovals on the left) and modify their sensitivity to external ligand concentrations.

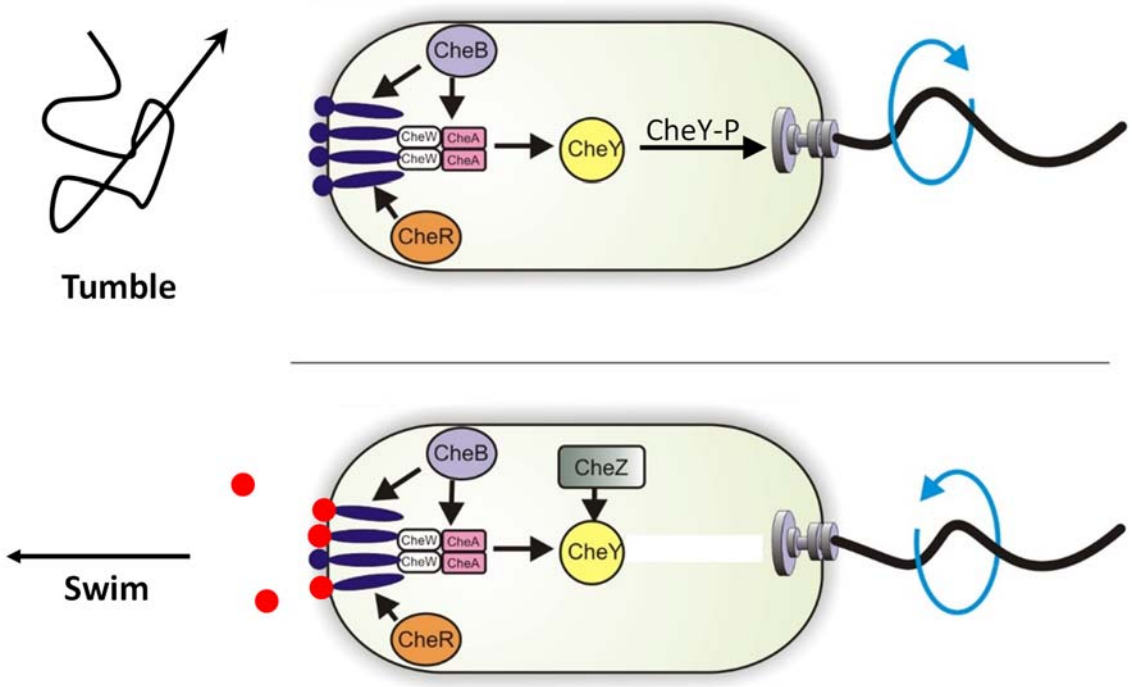

Figure 22.8. Phase diagrams for determining the equilibrium activity levels of interconvertible enzymes (I) subject to activation and inactivation cycles by enzymes F and R, respectively. The lines depict how the two rates change with increasing fraction of activated I. All points of intersection denote equilibria, but only the solid points are stable, as in these cases, deviations in both directions result in differences in activation and deactivation rates that return to the point. **Left**) With a system with no feedback, there is a single stable equilibrium. **Right**) When activated enzyme feeds back positively to the forward enzyme, the dynamics are altered in such a way that there can be as many as three equilibria, with the central one being unstable (deviations in either direction move the system to one of the alternative stable equilibria). Depending on the elevation and angularity of the activation curve, there might be only a single equilibrium in this case.